MODELING MULTIMODAL FAILURE EFFECTS OF COMPLEX SYSTEMS USING POLYWEIBULL DISTRIBUTION

THESIS

Daniel A. Timme, Capt, USAF

AFIT-ENV-MS-18-M-239

DEPARTMENT OF THE AIR FORCE
AIR UNIVERSITY

AIR FORCE INSTITUTE OF TECHNOLOGY

Wright-Patterson Air Force Base, Ohio

DISTRIBUTION STATEMENT A.
APPROVED FOR PUBLIC RELEASE; DISTRIBUTION UNLIMITED.

The views expressed in this thesis are those of the author and do not reflect the official policy or position of the United States Air Force, the Department of Defense, or the United States Government. This material is declared a work of the U.S. Government and is not subject to copyright protection in the United States.

AFIT-ENV-MS-18-M-239

MODELING MULTIMODAL FAILURE EFFECTS OF COMPLEX SYSTEMS USING POLYWEIBULL DISTRIBUTION

THESIS

Presented to the Faculty

Department of Systems Engineering and Management

Graduate School of Engineering and Management

Air Force Institute of Technology

Air University

Air Education and Training Command

in Partial Fulfillment of the Requirements for the

Degree of Master of Science in Systems Engineering

Daniel A. Timme, B.S.Math, B.S.B.M.

Capt, USAF

March 2018

DISTRIBUTION STATEMENT A.
APPROVED FOR PUBLIC RELEASE; DISTRIBUTION UNLIMITED.

AFIT-ENV-MS-18-M-239

MODELING MULTIMODAL FAILURE EFFECTS OF COMPLEX SYSTEMS USING POLYWEIBULL DISTRIBUTION

Daniel A. Timme, B.S.Math, B.S.B.M.
Capt, USAF

Committee Membership:

Maj Jason K. Freels , Ph.D.
Chair

Lt Col Richard S. Seymour, Ph.D.
Member

Maj Thomas P. Talafuse, Ph.D.
Member

AFIT-ENV-MS-18-M-239

Abstract

The Department of Defense (DoD) enlists multiple complex systems across each of their departments. Between the aging systems going through an overhaul and emerging new systems, quality assurance to complete the mission and secure the nation‘s objectives is an absolute necessity. The U.S. Air Force‘s increased interest in Remotely Piloted Aircraft (RPA) and the Space Warfighting domain are current examples of complex systems that must maintain high reliability and sustainability in order to complete missions moving forward. DoD systems continue to grow in complexity with an increasing number of components and parts in more complex arrangements. Bathtub-shaped hazard functions arise from the existence of multiple competing failure modes which dominate at different periods in a systems lifecycle. The standard method for modeling the infant mortality, useful-life, and end-of-life wear-out failures depicted in a bathtub-curve is the Weibull distribution. However, this will only model one or the other, and not all three at once. The poly-Weibull distribution arises naturally in scenarios of competing risks as it describes the minimum of several independent random variables where each follows a distinct Weibull law. Little is currently known or has been developed for the poly-Weibull distribution. In this report, the poly-Weibull is compared against other goodness-of-fit models to model these completing multimodal failures. An equation to determine the moments for the poly-Weibull is derived leading to the development of properties such as the mean, variance, skewness, and kurtosis using Maximum Likelihood Estimation (MLE) parameters obtained from a data set with known bathtub shaped hazard function.

Para mi esposa - que el amor y el apoyo es el vinculo que mantuvo todo junto. Tus constante apoyo es lo que hizo todo esto posible. Soy un hombre mejor gracias a ti.
To my daughter - my life changed the first time I held you. You have always been my motivation to achieve more than I knew was possible.
To my parents - Thank you for everything. Your love, support, and dedication has provided me with a solid foundation for which I can build my future.

Acknowledgements

I would like to thank individuals in the Department of Mathematics and Statistics and the Department of Operational Sciences for all of their assistance with this research paper. I would like to thank everyone who took the time to proofread this paper and offered not only grammatical advice, but professional and structural advice as well. Thank you to all the members of my thesis committee for your guidance. Also, I would like to thank my advisor for presenting this problem to solve and all of the assistance along the way. Thank you all for your patience and willingness to teach.

Daniel A. Timme

Table of Contents

Page

Abstract iv

Dedication v

Acknowledgements vi

Table of Contents vii

List of Figures ix

List of Tables x

I. Introduction 1

II. Literature Review 13

2.1 Importance to DoD 13
2.2 Modified Weibull Distributions 18
2.2.1 Additive Weibull Distribution 18
2.2.2 Modified Weibull Distribution 19
2.2.3 Beta Modified Weibull Distribution 20
2.2.4 New Modified Weibull Distribution 21
2.2.5 Exponentiated Modified Weibull Extension 22
2.2.6 poly-Weibull Distribution 23
2.3 Weibull Comparison 24
2.4 Closed-Form Derivation of poly-Weibull Moments 26

III. Methodology 33

3.1 Derivation of bi-Weibull Moments 34
3.1.1 Uniform Convergence Proof 36

IV. Results 41

4.1 Statistical Properties of poly-Weibull moments 43
4.1.1 Mean & Standard Deviation 44
4.1.2 Variance 46
4.1.3 Skewness 47

Page

4.1.4 Kurtosis 48
4.1.5 Obtained Values 50
4.2 Computational Testing 51

V. Conclusion & Future Work 57

5.1 Conclusion 57
5.2 Future Work 57

Appendix A: Math Tools & Extra Derivations 59

Appendix B: Code 68

Appendix C: List of Acronyms 94

Bibliography 95

Vita 97

List of Figures

Figure Page

1.1 Series Example 2

1.2 Parallel Example 3

1.3 Basic Series/Parallel Examples 4

1.4 Generic Combined Series/Parallel Example 5

1.5 Generic Complex Series/Parallel Example 6

1.6 Generic Complex Series/Parallel Subsystem Example 7

1.7 Serial Flaws 7

1.8 Bathtub-Curve Hazard Function 11

4.1 Convergence of bi-Weibull & tri-Weibull Mean & Standard Deviation 44

4.2 Convergence of tri-Weibull Mean & Standard Deviation Inner Sum 45

4.3 Convergence of bi-Weibull & tri-Weibull Outer Variance 46

4.4 tri-Weibull Variance Inner Sum 47

4.5 Convergence of bi-Weibull Skewness 47

4.6 Convergence of tri-Weibull Inner & Outer Sum Skewness 48

4.7 Convergence of bi-Weibull Kurtosis 49

4.8 Convergence of tri-Weibull Inner & Outer Sum Kurtosis 49

4.9 bi-Weibull & tri-Weibull PDF 51

4.10 Comparing model fit for the Aarset data 53

4.11 bi-Weibull, tri-Weibull, EMWE, & NMW PDF 56

List of Tables

Table Page

2.1 Weibull Shape Parameters 16

2.2 The Aarset Data Set 25

2.3 PDF for Weibull Distributions 25

4.1 First 4 raw moments for bi-Weibull & tri-Weibull 41

4.2 bi-Weibull & tri-Weibull MLE's for the Aarset Data Set 43

4.3 tri-Weibull Mean, Variance, & Standard Deviation 50

4.4 Performance Measures for the Aarset Data Set 52

4.5 MLE's for the Aarset Data Set 54

4.6 Modified Weibull Raw Moment Values 54

4.7 Modified Weibull Properties 55

MODELING MULTIMODAL FAILURE EFFECTS OF COMPLEX SYSTEMS USING POLYWEIBULL DISTRIBUTION

I. Introduction

The United States Department of Defense (DoD) acquires and supports many complex systems each containing multiple potential failure modes. Many aging systems are undergoing an overhaul while numerous new systems are simultaneously emerging. Reliability of these systems ensures mission success, which results in multiple cost savings. The warfighting domain is changing and defense systems will continue to grow in complexity, which suggests that the number of embedded potential failure modes will also increase. In an effort to maintain its standing as the dominant military leader and protect the nation‘s interests, the United States will need to be prepared and ensure all defense systems are reliable and fully functional to complete the mission, despite the increasing complexity and challenges that lie ahead.

Reliability is defined as the probability that a component or system will perform a required function for a given period of time when used under stated operating conditions. Mathematically, this is expressed by the reliability function, $R(t)$, as

$$R(t) = Pr(T > t) \ni T \geq 0 \tag{1.1}$$

where t is the time of interest. Since a system must be in either failed state or a working state at time t, the probability that a failure occurs before a time t is given by

$$F(t) = 1 - R(t), \tag{1.2}$$

known as the Cumulative Distribution Function (CDF). The Probability Density Function (PDF) (where it exists) is simply the derivative of the CDF,

$$f(t) = \frac{d}{dt}F(t) \tag{1.3}$$

From the PDF and Reliability function, the hazard function can be determined. The hazard function is defined as:

$$h(t) = \frac{f(t)}{R(t)} \tag{1.4}$$

Ebeling [1] states that the definition of system reliability must be made specific to determine reliability, in the operational sense. By that, he says that an unambiguous and observable description of failure must be established, a unit of time must be identified, and the system should be observed under normal performance. For systems, reliability can be found by first determining whether the system is in series or parallel. A system is considered series when all components must operate in a satisfactory manner if the system is to function properly [2]. The common diagram is shown in Figure 1.1.

Figure 1.1: Series Example

where R_1, R_2, R_N is the reliability of each respective component. Eq. 1.5 is used to determine the reliability of a system in series.

$$R_s(t) = \prod_{i=1}^{n} R_i(t) \tag{1.5}$$

A system is considered parallel when several of the same components are in parallel and each must fail to cause system failure. A common diagram for a system in parallel is shown in Figure 1.2.

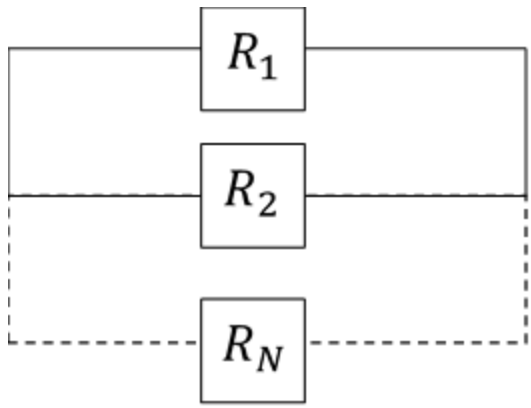

Figure 1.2: Parallel Example

where R_1, R_2, R_N is the reliability of each respective component. Components can be both in series and parallel. Eq. 1.6 is used to determine the reliability of a system in parallel.

$$R_p(t) = 1 - \prod_{i=1}^{n} [1 - R_i(t)] \tag{1.6}$$

For many systems, the subsystems are in any combination of series and parallel resulting in a combination of Eqs. 1.5 & 1.6. The more parallel components and subsystems that exist, the better the reliability. However, complex systems seldom exists in a parallel format. Each subsystem may have subsystems of their own, which are also in any combination of parallel and series all the way down to the component level. However, at the macro level everything tends to be in series, even if it is composed of multiple parallel subsystems. Consider a simple view of an aircraft, which consists of wings, an engine, a fuselage, a rudder, and controls. Each of these is a system by themselves with subsystems and components of their own, which are in series and parallel yet the aircraft depends on each of them. If any one of them fails, the aircraft may fail to perform its required function under its stated operating conditions.

Complex systems contain numerous subsystems and components with multiple failure modes. Each failure mode ultimately competes to see which occurs first and prevents the system from performing as it should; most failures tend to occur early or late

in the systems life. Complex systems ultimately operate as a series because they depend on so many pieces to function properly, that each parallel component does not impact the overall reliability by much. There are multiple dependencies throughout complex systems that any one component or subsystem failure ultimately leads to systems failure. Component reliability may be viewed with a simple diagram, such as any of the examples in Figure 1.3

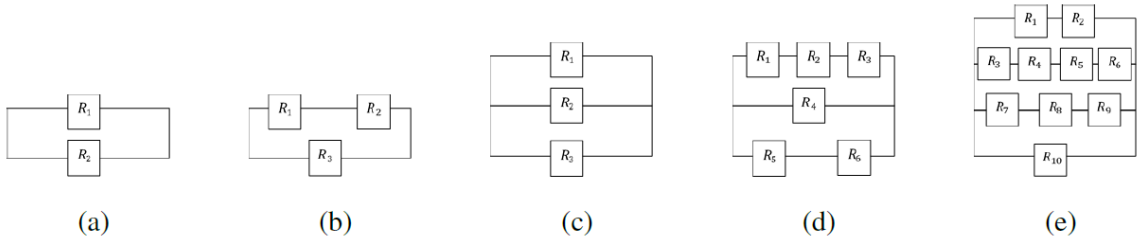

Figure 1.3: Basic Series/Parallel Examples

When the components are grouped into each subsystem, the diagrams grow in complexity as shown in Figure 1.4. A more complex component may have more fail-safes in the design. At this level, a parallel reliability model will have more impact. As complex components begin to be assembled into complex subsystems, these fail-safes become less apparent in the diagrams. As the subsystems are combined with other subsystems, this will become even more apparent.

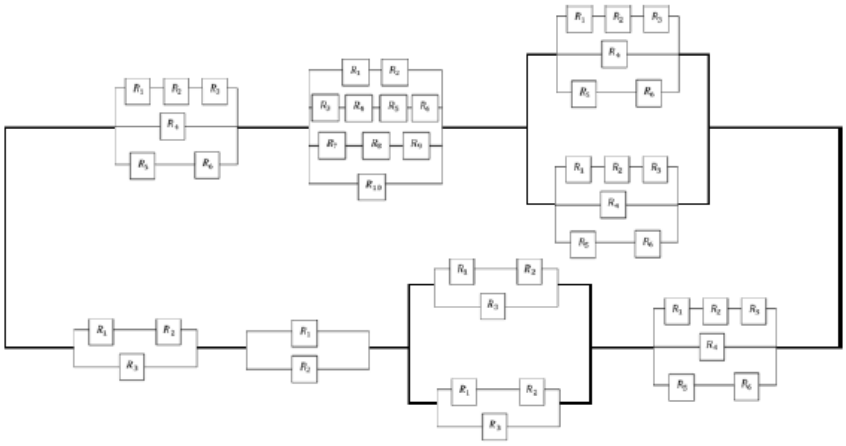

(a)

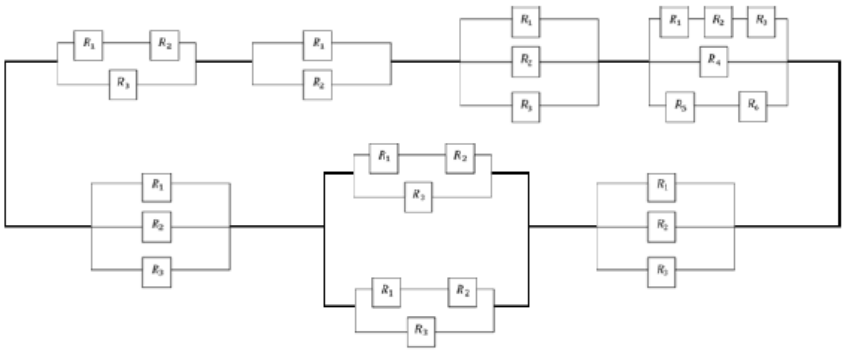

(b)

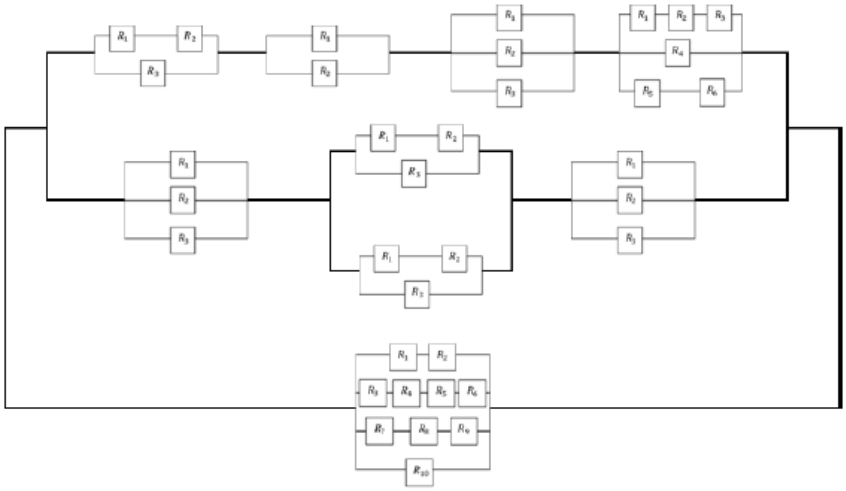

(c)

Figure 1.4: Generic Combined Series/Parallel Example

These subsystems will be grouped further into more subsystems such as those shown in Figure 1.5.

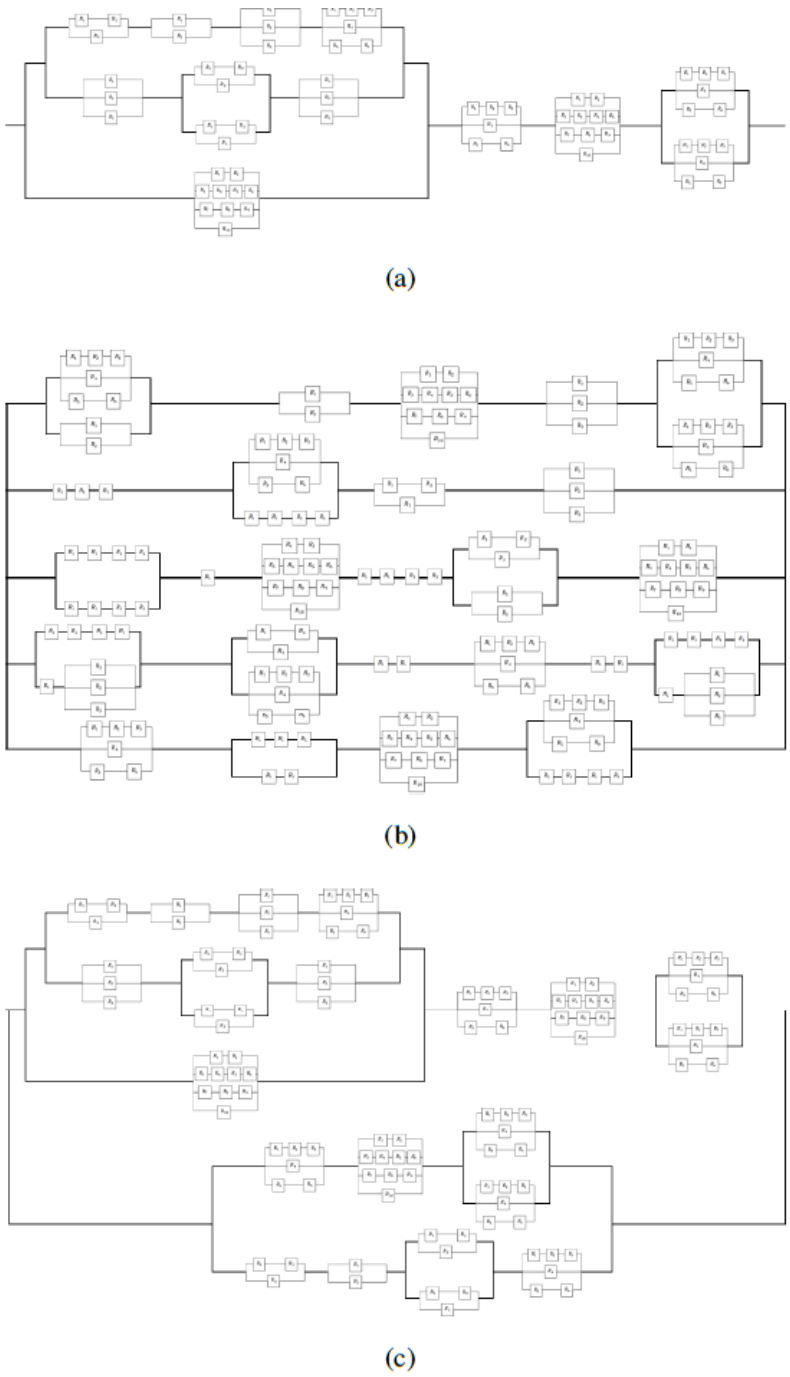

Figure 1.5: Generic Complex Series/Parallel Example

The more complex the system becomes, the more complex the diagram becomes (Figure 1.6). When the system is integrated, eventually the diagrams begin to show everything in series where each subsystem has a reliability of its own and the entire system is dependent on each subsystem.

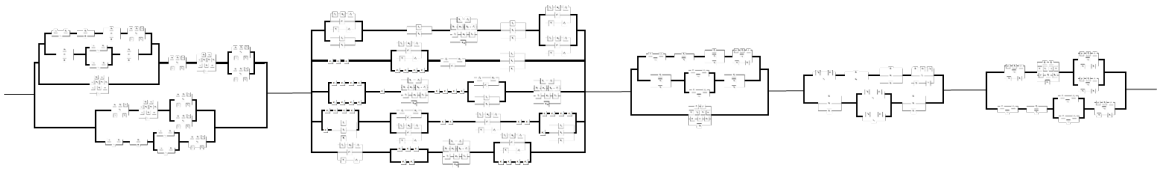

Figure 1.6: Generic Complex Series/Parallel Subsystem Example

Estimating system reliability from accelerated test data for systems with multiple failure modes requires adequate samples to observe each failure mode at multiple stress levels [3]; separate models may then be developed for each distinct failure mode. The exact reliability for the overall system can then be determined using Eq. 1.6. Figure 1.7 shows a serial arrangement of flaws within the prototypes subjected to qualitative accelerated reliability test. The arrangement demonstrates the competing risk assumption in the model where the time to failure for the prototype is the minimum activation time among the flaws.

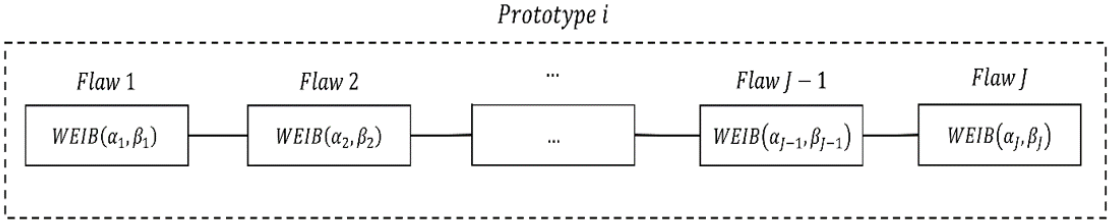

Figure 1.7: Serial Flaws

It is not common in qualitative testing that an appropriate number of prototypes are available to account for every possible failure mode that is yet to be discovered during early system testing. For tests conducted with limited sample sizes, an estimate of system reliability may be obtained by combining the observations of multiple failure modes to form a single distribution plot. In such a situation, an unknown number of independent flaws, denoted as J, compete to be the cause of system failure as shown in Figure 1.7. The observed lifetime for prototype i is therefore represented as the minimum occurrence time among the J modes in the system.

The DoD operates the most complex systems in the world in extreme environments with rapidly changing missions. It is vital that these systems are reliable. However, the DoD does not have a good track record of fielding reliable systems. Reliability growth is intended to identify and remove failure modes in developmental testing. Complex systems consist of multiple components with multiple working parts. Much of reliability entails quantifying these parts and/or subcomponents. However, if the systems do not perform as intended in the appropriate environment, this all results in a reliability of zero. Focusing too much on quantification of the parts in the beginning can cause cost overruns and lead to delays. Parts reliability is important, but parts failures aren't typically to blame for mission failure. In addition to classifying the appropriate parts, it is necessary to identify all possible failure modes and the potential outcome and mitigation strategies should that failure occur. Failure Modes Effects & Analysis (FMEA) is a qualitative method of identifying failure modes and determining the likelihood of occurrence and establishing potential mitigation strategies. It was listed in MIL-STD 1629A, though that was discontinued in 1994. There have been many variations of FMEA over the years but the concept remains the same. Pisacane describes FMEA in [4] as a bottom-up approach where low-level failure modes are postulated to determine higher-level effects. FMEA is recommended to increase reliability, improve designs and quality, while reducing costs.

M. Hurley Jr. and W. Purdy in [5] (p.366–375) refer to the parts reliability as a reliability prediction and how well the system performs in its operational environment as the true reliability. Further, they emphasize the importance of conducting a FMEA early in the system design and using that with the reliability prediction for mission success. Failure Mode, Effects, & Criticality Analysis (FMECA) is taken one step further than the traditional FMEA by quantifying it with probabilities; it was also part of MIL-STD 1629A. FMECA considers the criticality of each failure mode with respect to the successful completion of the mission and other standards [6]. This is not only an activity that can occur at the beginning of the design, FMEA/FMECA can be continuously applied as it evolves throughout the design of the system. These tools work well at the end of the process as well to continuously improve existing systems [2].

> "*The key to developing and fielding military systems with satisfactory levels of RAM is to recognize it as an integral part of the Systems Engineering process and to systematically manage the elimination of failures and failure modes through identification, classification, analysis, and removal or mitigation.*" DoD Guide For Achieving Reliability, Availability, and Maintainability [7]

Space systems undergo extensive environmental testing prior to launch to identify possible failures during transport and launch. Additionally, each subsystem will generally undergo environmental testing to certify that the system will be operational and able to complete the mission [5]. This is similar to the burn-in testing phase; however, space systems cannot be fully tested in the lab. FMEA plays an important role in identifying the potential failures for test.

Operational testing is just as (if not more) important than developmental testing as mentioned above. If a system cannot perform in the intended environment and complete its respective mission, then the system has no reliability at all. During operational test, the

system can experience failures from competing subsystems and other failure modes not identified during the developmental testing phase. Many systems continue to fail during operational testing despite the developmental testing they had undergone.

Often times, over-simplified models are used to predict system reliability which are not capable of modeling complex systems with multiple failure modes. This becomes apparent during the operational testing phase of a system, or in some cases, when the system has become fully operational. There are multiple models that can model multiple events that exist within a system. The focus of this paper will be to compare some of the current methods with the poly-Weibull method.

Despite its shortcomings, the Weibull distribution has been regarded as one of the most useful distributions in reliability [1], leading to the creation of many alternate forms. Weibull has been successful with modeling constant or monotone, increasing or decreasing hazard functions. These, however, are not common with complex systems, which tend to have multiple failure modes resulting in non-monotone hazard functions and ultimately in what is commonly referred to as a bathtub-curve.

A bathtub-curve (shown in Figure 1.8 [6]) is a useful conceptual model for the hazard function which shows how products may encounter a majority of the failures either early or late in their lifetime; with the focus of many reliability studies often being only one or the other side of the curve [6]. The bathtub-curve is cited in multiple textbooks covering reliability and maintainability engineering. That being said, there are many who doubt the overall usefulness of the bathtub-curve to model systems. One group of authors outline [8] certain cases where the bathtub-curve fails to accurately model the hazard function. In the article, they provide empirical evidence which suggests where the bathtub-curve fails, and cite several sources that outline arguments against the bathtub-curve and the usefulness of burn-in testing. However, many firms and government agencies have used burn-in testing

and methods to model their failures with the bathtub-curve, and it continues to be widely cited and utilized in manufacturing and warranty planning.

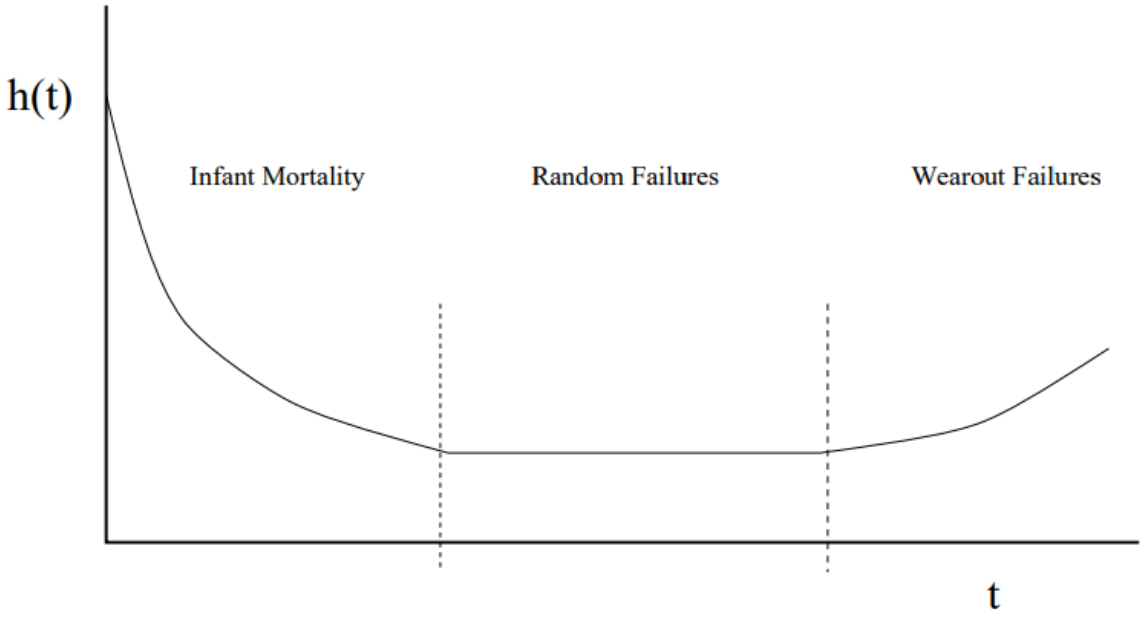

Figure 1.8: Bathtub-Curve Hazard Function

The early failures (often referred to as infant mortality) demonstrate a decreasing failure rate (DFR). These are followed by a nearly constant failure rate (CFR) where random failures occur, known as the useful life. Lastly, the product will undergo an increasing failure rate (IFR) known as wearout failures during the end-of-life of the product [1]. The curve can be demonstrated by a composite of multiple failure distributions, or even as a function of piecewise linear and CFR‘s [1]. This, however, could be quite cumbersome when trying to model system reliability. The burden of modeling the reliability with a composite of multiple failure distributions, or as a piecewise function of linear and constant failure rates would greatly increase with complex multimodal failure systems. There are several methods that have been presented to model the bathtub-curve, many of them centered on the popular Weibull distribution.

To model a bathtub-curve the equations would need to be decreasing from time $t = t_0$ and contain at least one minimum point eventually increasing as $t \to \infty$. Several methods have been presented to model bathtub failures, however, since the Weibull does a great job modeling lifetime failure rates, modifications of this form will be examined in this paper.

II. Literature Review

2.1 Importance to DoD

Delays and cost overruns continually plague the DoD as funding resources made available to operate and maintain system can fluctuate from year to year. This fluctuation provides motivation to implement reliability models and testing strategies to mitigate these delays and cost overruns. According to [7], the most important Reliability, Availability, & Maintainability (RAM) activity is to identify potential failures and make necessary design changes to remove these modes during the system development phase. Reliability models and proper identification of failure modes will help ensure the design satisfies the requirements. The cost of implementing system redesigns late in the program can be reduced when resources are properly allocated and proper testing is achieved. Testing helps address potential failure modes that may lead to mission failure and discover appropriate mitigation strategies. Several studies of DoD systems were reviewed in [7]. A few of the cited reasons why systems fail to achieve RAM requirements are failure to implement reliability early in the development process, inadequate lower level testing at component or subcomponent level, inadequate planning for reliability, and ineffective implementation of reliability tasks in improving reliability. In the time since these reviews were performed, DoD acquisition systems have become more complex and will continue to grow in complexity in the future. More systems are being designed with new digital and electronic intricacies. Guidance has been provided by the DoD in numerous documents, including [9] and [10]. These standards specify a scientific approach to design and build reliability into products early on and institutionalize the creation of a comprehensive reliability growth strategy throughout the acquisition cycle.

The Fiscal Year (FY) 2018 DoD budget amounts to $208.6 billion. This cost includes $125.2 billion for Procurement funded programs and $83.3 billion for Research,

Development, Test, & Evaluation (RDT&E) funded programs; directly relating to reliability systems. In the FY 2018 projected budget, $94.9 billion has been allocated towards supporting programs that have been designated as Major Defense Acquisition Programs (MDAPs) [11]. Of the $83.3 billion going to RDT&E, $13.2 billion is scheduled for Science & Technology (S&T). Particular attention should be given to space systems within DoD. For the most part, these systems do not undergo maintenance once they become operational. In particular, spacecraft cannot be retrieved for diagnostics or repair [4]. Space system designs become very complex and expensive in their ongoing effort to achieve amazing endeavors [12]. In order to achieve these feats, everything needs to work to achieve mission success. Space based systems amount to $9.8 billion in the FY 2018 budget, up from $7.1 billion in FY 2017 ([11] [13]).

> "*The space industry's understanding of, and approach to, reliability can be one of the most important drivers of a programs cost and schedule*" M. Hurley & W. Purdy in [5] p. 366

The U.S. Navy commissioned the USS Gerald Ford (CVN 78) on 22 July 2017; the first new class of aircraft carriers in 40 years ([14] [15] [16]). The mission of the new class of aircraft carriers is to provide "The United States with the core capabilities for forward presence, deterrence, sea control, power projection, maritime security and humanitarian assistance. The Gerald R. Ford class will be the premier forward asset for crisis response and early decisive striking power in a major combat operation" [11]. The carrier is largely automated, reducing the required crew from the Nimitz class by approximately 600 ([14] [16]). The new Ford class of aircraft carrier has several new state-of-the-art technological advances such as Electromagnetic-Powered Aircraft Launch System (EMALS), Advanced Arresting Gear (AAG) system, reduced heat signatures, and several quality of life improvements for the crew [17]. The technology upgrades from the Nimitz class are stated such that the ship can essentially drive itself ([14] [15] [16]). Recall the the

definition of reliability, the probability to perform some function for a given period of time when used under the stated conditions. If EMALS or AAG fails, the aircraft carrier cannot take off or land aircraft; if it cannot perform it's function then then it cannot complete the mission and thus has a reliability of zero.

These new complex DoD systems will rely more heavily on reliability models to better predict and plan for failures, resulting in cost savings and a lessened impact on the mission. More reliable models will allow better planning for maintenance, thus extending the useful life of the system. CVN 78 is currently still undergoing testing and is expected to become deployable by 2020. It will be closely followed by more Ford class aircraft carriers as President Trump has stated that he would like to increase the U.S. Navy's aircraft carrier fleet from 11 to 12 [14]. In 2011, Congress mandated a requirement of a minimum of 11 aircraft carriers. FY 2018 budget allocates $30.4 billion to ship building and maritime systems ($27 billion FY 2017), which includes construction cost for the first year of USS Enterprise (CVN 80) and final year of the USS John F. Kennedy (CVN 79) ([11] [13]). With the expected increase in Naval assets and increased complexities of the ships, reliability and maintainability will need to be a strong consideration to ensure mission success and prevent delays and cost overruns.

As stated in Chapter 1, complex systems are composed of multiple parts and components structured in complex arrangements; each having it's own independent failure mode and distribution associated with it. Certain failures may dominate during certain periods of the systems lifecycle which leads to the bathtub shaped hazard function in Figure 1.8. The Weibull distribution has been used to model complex systems such as the CVN 78. However, it is often used incorrectly as each failure mode follows a distinct Weibull law as illustrated in Figure 1.7.

The Weibull distribution was introduced in 1939 by the Swedish physicist Waloddi Weibull; he discusses a number of applications in [18] published in 1951.The Weibull

distribution has been regarded as one of the most useful distributions in reliability [1]. However, the distribution has shortcomings that have led to the development of many alternate forms.

Table 2.1: Weibull Shape Parameters

Value	**Property**
$0 < \beta < 1$	DFR
$\beta = 1$	CFR, Exponential Distribution
$1 < \beta < 2$	IFR, Concave
$\beta = 2$	LFR, Rayleigh Distribution
$\beta > 2$	IFR, Convex
$3 \leq \beta \leq 4$	IFR, Approaches Normal Distribution; symmetrical

In this paper, the Weibull distribution is expressed with parameters β and α where β is a shape parameter and α is a scale parameter. Table 2.1 shows what different values of the shape parameter may represent. Recall in Chapter 1 how Figure 1.8 illustrated the bathtub-curve with three phases where each of the three phases was driven by DFR, CFR, & IFR. Table 2.1 demonstrate how the value for β can lead to the bathtub-shaped hazard function with enough shape parameters.

$$f(t|\alpha,\beta) = \frac{\beta}{\alpha}\left(\frac{t}{\alpha}\right)^{\beta-1} \exp\left[-\left(\frac{t}{\alpha}\right)^{\beta}\right] \tag{2.1}$$
$$\ni \alpha,\beta > 0, \quad t \geq 0$$

and

$$F(t|\alpha,\beta) = 1 - \exp\left[-\left(\frac{t}{\alpha}\right)^{\beta}\right] \tag{2.2}$$

$$\ni \alpha,\beta > 0, \quad t \geq 0. \tag{2.3}$$

The expected value equation for the Weibull Distributions is given as:

$$E\left[t^k\right] = \alpha\Gamma\left(1 + \frac{1}{\beta}\right) \tag{2.4}$$

$$\ni \alpha,\beta > 0, \quad t \geq 0$$

where $\Gamma(t)$ is the gamma function and is given by $\Gamma(k) = \int_0^\infty t^{k-1}\exp[-t]dt$. The expected value equation can be used to determine the first four raw moments which is used to determine statistical properties such as the mean (μ), variance ($Var[t]$), skewness ($Sk[t]$), and kurtosis ($\kappa[t]$). The standard deviation is determined from the variance using $\sigma = \sqrt{Var[t]}$. In reliability, the mean is often referred to as the Mean Time to Failure (MTTF). These statistical properties are given in Eqs. 2.5, 2.6, 2.7, & 2.8 shown below.

$$\text{MTTF} = \mu = \alpha\Gamma\left(1 + \frac{1}{\beta}\right) \tag{2.5}$$

$$\ni \alpha,\beta > 0, \quad t \geq 0$$

$$Var[t] = \alpha^2\left\{\Gamma\left(1 + \frac{2}{\beta}\right) - \Gamma\left(1 + \frac{1}{\beta}\right)^2\right\} = \sigma^2 \tag{2.6}$$

$$\ni \alpha,\beta > 0, \quad t \geq 0$$

$$Sk[t] = \frac{\Gamma\left(1 + \frac{3}{\beta}\right)\alpha^3 - 3\mu Var[t] - \mu^3}{\sigma^3} \tag{2.7}$$

$$\ni \alpha, \beta > 0, \quad t \geq 0$$

$$\kappa[t] = \frac{\Gamma\left(1 + \frac{4}{\beta}\right)\alpha^4 - 4Sk[t]\sigma^3\mu - 6\mu^2 Var[t] - \mu^4}{\sigma^4} - 3 \tag{2.8}$$

$$\ni \alpha, \beta > 0, \quad t \geq 0$$

The two-parameter Weibull is sufficient for modeling data produced from individual failure modes that may be defined as either infant-mortality, useful-life or end-of-life causes. The Weibull distribution has had great success with modeling failure rates for which the hazard function is either constant or monotone-increasing or decreasing [6]. When $\beta = 1$, the failure rate is constant and equal to the scale parameter (α) . When $\beta > 1$, the failure rate increases proportionally with time indicating that the failure occurs later in the system's life, often due to wear-out. When $\beta < 1$, the failure rate decreases proportionally with time indicating that failure is more likely to occur early in the system's life due to a design or manufacturing flaw; this is commonly referred to as infant-mortality. These, however, are not common with complex systems which tend to have multiple failure modes resulting in non-monotone hazard functions. Several modifications to the Weibull distribution have been developed to model such failure data, several of these modified distributions are presented in the following section.

2.2 Modified Weibull Distributions

2.2.1 Additive Weibull Distribution.

One particular method presented by Min Xie and Chin Diew Lai in 1995 is known as the additive Weibull distribution. The concept behind this model is to combine two Weibull distributions; one with an increasing failure rate and the other with a decreasing failure rate [19]. Using the same shape and scale parameters, the PDF and CDF are expressed as,

$$f(t|\alpha_1,\alpha_2,\beta_1,\beta_2) = \left(\frac{\beta_1}{\alpha_1}(\alpha_1 t)^{\beta_1-1} + \frac{\beta_2}{\alpha_2}(\alpha_2 t)^{\beta_2-1}\right)\exp\left[-(\alpha_1 t)^{\beta_1} - (\alpha_2 t)^{\beta_2}\right]$$
$$\ni \alpha_1,\beta_1,\alpha_2.\beta_2 > 0, \quad t \geq 0 \tag{2.9}$$

and

$$F(t|\alpha_1,\alpha_2,\beta_1,\beta_2) = 1 - \exp\left[-(\alpha_1 t)^{\beta_1} - (\alpha_2 t)^{\beta_2}\right]$$
$$\ni \alpha_1,\beta_1,\alpha_2,\beta_2 > 0, \quad t \geq 0. \tag{2.10}$$

The additive Weibull does not have a closed form to the integral for the mean or variance; numerical integration is the method suggested in [19] and [20]. Usgaonkar and Mariappan provide highlights from three case studies using the additive Weibull distribution in [20].

2.2.2 Modified Weibull Distribution.

Another model is the Modified Weibull (MW) Distribution presented in [21] in 2003 by Lai, Xie, and Murthy. This method was derived using a three parameter model and it stated as being a limiting case of the Beta Integrated Model [21].

The PDF is:

$$f(t|\alpha,\beta,\lambda) = \lambda\beta\left(\frac{t}{\alpha}\right)^{\beta-1}\exp\left[\left(\frac{t}{\alpha}\right)^{\beta} + \lambda\alpha\left(1 - \exp\left[\left(\frac{t}{\alpha}\right)^{\beta}\right]\right)\right]$$
$$\ni \lambda,\alpha,\beta > 0 \quad t \geq 0 \tag{2.11}$$

The CDF is:

$$F(t|\alpha,\beta,\lambda) = 1 - \exp\left[\lambda\alpha\left(1 - \exp\left[\left(\frac{t}{\alpha}\right)^{\beta}\right]\right)\right]$$
$$\ni \lambda,\alpha,\beta > 0 \quad t \geq 0 \tag{2.12}$$

where β is the shape parameter, α is a scale parameter, and λ is an accelerating factor that Silva et al., state that "it works as a factor of fragility in the survival of the individual when the time increases" [22]. Just as with the additive Weibull, the modified Weibull does not have a closed form solution for the mean and variance and thus they must be solved for using numerical integration or other methods. The modified Weibull distribution is asymptotically related to the Weibull and exponential distributions and can be estimated easily either statistically or on Weibull Probability Paper (WPP) plot [21].

2.2.3 Beta Modified Weibull Distribution.

The Beta Modified Weibull (BMW) distribution was introduced by Silva, Ortega, and Cordeiro; published in *Lifetime Data Analysis* in 2010. The BMW distribution is comprised of many significant distributions including the generalized beta Weibull, exponentiated Weibull, beta exponential, MW and Weibull distributions; all as special submodels of the BMW [22]. Throughout their journal article, Silva et al. consistently reference the relationship of the BMW to the MW Distribution discussed earlier; the CDF contains the MW as a limit of integration. This model uses a five-parameter distribution with β as the shape parameter, α as the scale parameter, and λ as the accelerating factor. The model also contains the Beta Distribution, given as

$$B(t|a,b) = \int_0^1 t^{a-1}(1-t)^{b-1}dt = \frac{\Gamma(a)\Gamma(b)}{\Gamma(a+b)} \quad a,b > 0 \tag{2.13}$$

The PDF and CDF are given as,

$$f(t|\alpha,\beta,\lambda,a,b) = \frac{\alpha t^{\beta-1}(\beta+\lambda t)\exp[\lambda t]}{B(a.b)}\left(1-\exp\left[-\alpha t^{\beta}\exp[\lambda t]\right]\right)^{a-1} exp\left[-b\alpha t^{\beta}\exp[\lambda t]\right]$$
$$\ni t,\alpha,\beta,a,b > 0 \quad \lambda \geq 0 \tag{2.14}$$

and

$$F(t|\alpha,\beta,\lambda,a,b) = \frac{1}{B(a,b)} \int_0^{1-\exp\left[\lambda\alpha\left(1-\exp\left[\left(\frac{t}{\alpha}\right)^{\beta}\right]\right)\right]} \omega^{a-1}(1-\omega)^{b-1}d\omega$$

$$\ni t,\alpha,\beta,a,b > 0 \quad \lambda \geq 0, \tag{2.15}$$

respectively. In contrast to the standard Weibull, the BMW distribution accommodates monotone, unimodal and bathtub-shaped hazard functions and therefore can successfully be utilized in the analysis of survival data. The BMW distribution has seventeen special case distributions for which many can be tested for goodness of fit by it [22].

2.2.4 New Modified Weibull Distribution.

Almalki and Yuan [23] introduced the New Modified Weibull (NMW) distribution in 2013 with PDF and CDF

$$f(t|\alpha_1,\alpha_2,\beta_1,\beta_2,\lambda) = \left(\alpha_1\beta_1 t^{\beta_1-1} + \alpha_2\left(\beta_2+\lambda t\right)t^{\beta_2-1}\exp\left[-\lambda t\right]\right)\exp\left[-\alpha_1 t^{\beta_1} - \alpha_2 t^{\beta_2}\exp[\lambda t]\right]$$

$$\ni \alpha_1,\beta_1,\alpha_2,\beta_2,\lambda \geq 0 \quad t \geq 0 \tag{2.16}$$

$$F(t|\alpha_1,\alpha_2,\beta_1,\beta_2,\lambda) = 1 - \exp\left[-\alpha_1 t^{\beta_1} - \alpha_2 t^{\beta_2}\exp[\lambda t]\right]$$

$$\ni \alpha_1,\beta_1,\alpha_2,\beta_2,\lambda \geq 0 \quad t \geq 0, \tag{2.17}$$

respectively, by considering a two-component serial arrangement in which one component follows a standard two-parameter Weibull model and the other follows a MW distribution [21]. Similar to the BMW model, the NMW model simplifies into several other models; three of which are the standard Weibull, MW, and additive Weibull. It simplifies to a standard Weibull when $\alpha_2 = \beta_2 = \lambda = 0$, an additive Weibull when $\lambda = 0$, and MW when $\alpha_1 = \beta_1 = 0$ [21]. The NMW is increasing when $\beta_1,\beta_2 \geq 1$ and decreasing when $\beta_1,\beta_2 < 1$ and $\lambda = 0$. The NMW hazard function will generate a bathtub-curve, when neither the

increasing nor decreasing parameters are true [21]. Like the other modified Weibull distributions, the NMW distribution does not have a closed for solution to 2.18 in deriving the moments. Almaki and Yuan [23] were able to derive the moments using a Taylor-Series Expansion as shown in Eq. (2.19)

$$E\left[t^k\right] = \int_0^\infty kt^{k-1} \exp\left[\alpha_1 t^{\beta_1} - \alpha_2 t^{\beta_2} \exp[[\lambda t]]\right] dt \tag{2.18}$$

$$E[t^k] = \frac{k}{\theta} \sum_{n=0}^{\infty} \sum_{m=0}^{\infty} \frac{(-\alpha_2)^n (\lambda n)^m}{n!m!} \alpha_1^{-(n\beta_2+m+k)/\beta_1} \Gamma\left(\frac{n\beta_2 + m + k}{\beta_2}\right) \tag{2.19}$$

where $k \in \mathbb{Z}^+$

From here, one could determine the first four raw moments from either equation by setting $k = 1, 2, 3, 4$ to determine the mean, variance, skewness, and kurtosis.

2.2.5 Exponentiated Modified Weibull Extension.

The Exponentiated Modified Weibull Extension (EMWE) [24] is a four parameter distribution with scale parameters, α_1, α_2 and shape parameters β_1, β_2 that can be generalized into several other Weibull distributions, including the MW [21] presented by Xie et al. This Weibull distribution was introduced by Sarhan and Apaloo [24] in 2013 with PDF and CDF given by Eq. (2.20) and Eq. (2.21), respectively. The EMWE is increasing when $\beta_1, \beta_2 \geq 1$ and forms a bathtub shape when $\alpha_2 < 1$ for any value of β_1 or $\beta_1 < 1$ for any value of α_2.

$$\begin{aligned} f(t|\alpha_1, \alpha_2, \beta_1, \beta_2) = {} & \alpha_2\beta_1\beta_2\left(\frac{t}{\alpha_1}\right)^{\beta_1-1} \exp\left[\left(\frac{t}{\alpha_1}\right)^{\beta_1} + \alpha_1\alpha_2\left(1 - \exp\left[\left(\frac{t}{\alpha_1}\right)^{\beta_1}\right]\right)\right] \\ & \times \left[1 - \exp\left[\alpha_1\alpha_2\left(1 - \exp\left[\left(\frac{t}{\alpha_1}\right)^{\beta_1}\right]\right)\right]^{\beta_2}\right]^{\beta_2-1} \\ & \ni \alpha_1, \alpha_2, \beta_1, \beta_2 > 0 \quad t \geq 0 \end{aligned} \tag{2.20}$$

$$F\left(t|\alpha_1,\alpha_2,\beta_1,\beta_2\right) = 1 - \exp\left[\alpha_1\alpha_2\left(1 - \exp\left[\left(\frac{t}{\alpha_1}\right)^{\beta_1}\right]\right)\right]^{\beta_2}$$
$$\ni \alpha_1,\alpha_2,\beta_1,\beta_2 > 0 \qquad t \geq 0 \tag{2.21}$$

Just as the previous methods, there is not a closed form solution for the moments (Eq. 2.22) and numerical methods would be required to determine the raw moments. The authors use numerical methods with Eq. 2.23 to generate plots for the skewness and kurtosis by varying the value of β_2.

$$E\left[t^k\right] = \frac{\lambda\alpha_2\beta_2}{\alpha_1^{\beta_1-1}}\int_0^\infty t^{k+\alpha_2-1}\exp\left[(t/\alpha_1)^{\alpha_2} + \lambda\alpha_1\left(1 - \exp\left[(t/\alpha_1)^{\alpha_2}\right]\right)\right] \tag{2.22}$$
$$\times\left[1 - \exp\left[\lambda\alpha_1\left(1 - \exp\left[(t/\alpha_1)^{\alpha_2}\right]\right)\right]\right]^{\beta_2-1}$$

Eq. 2.22 can be represented in terms of the MW distribution:

$$E\left[t^k\right] = \sum_{j=0}^{\infty}\frac{(-1)^j\Gamma(\beta_2+1)}{\Gamma(\beta_2 j)(j+1)!}\int_0^\infty t^k f_{MW}(t;(j+1)\alpha_1,\alpha_2,\beta_1)dt$$

By using the moments for the MW distribution, $E\left[t^k\right]_{MW} = \int_0^\infty t^k f_{MW}\left(t;(j+1)\alpha_1,\alpha_2,\beta_1\right)$, $E\left[t^k\right]$ can be written as:

$$E\left[t^k\right] = \sum_{j=0}^{\infty}\frac{(-1)^j\Gamma(\beta_2+1)}{\Gamma(\beta_2 j)(j+1)!}E\left[t^k\right]_{MW} \tag{2.23}$$

2.2.6 poly-Weibull Distribution.

The poly-Weibull was introduced over twenty years ago by Berger and Sun [25]. The PDF of the poly-Weibull distribution is expressed as:

$$f\left(t|\alpha_j,\beta_j\right) = \exp\left[-\sum_{j=1}^{J}\left(\frac{t}{\alpha_j}\right)^{\beta_j}\right]\left[\sum_{j=1}^{J}\frac{\beta_j t^{\beta_j-1}}{\alpha_j^{\beta_j}}\right] \tag{2.24}$$

where $J \in \mathbb{Z}^+$ and α_j,β_j represent the scale and shape parameters associated with the Weibull model describing risk $j = 1, 2, , J$. Accordingly, the poly-Weibull CDF is expressed as

$$F\left(t|\alpha_j,\beta_j\right) = 1 - \exp\left[-\sum_{j=1}^{J}\left(\frac{t}{\alpha_j}\right)^{\beta_j}\right] \tag{2.25}$$

When $J = 2$, equations (2.24) and (2.25) are the CDF and PDF of the bi-Weibull distribution, and when $J = 3$ the model is naturally known as the tri-Weibull distribution. A value for $\beta_j < 1$ implies a decreasing hazard rate indicating infant mortality while a value for $\beta_j > 1$ infers a wear-out failure mechanism with an increasing hazard rate function. The poly-Weibull distribution is therefore capable of modeling data with bathtub shaped hazard functions by fitting multiple failure processes simultaneously. The raw moments for the poly-Weibull can be determined from Eq. 2.26.

$$E\left[t^k\right] = \int_0^\infty t^k \exp\left[-\sum_{j=1}^{J}\left(\frac{t}{\alpha_j}\right)^{\beta_j}\right]\left[\sum_{j=1}^{J}\frac{\beta_j t^{\beta_j-1}}{\alpha_j^{\beta_j}}\right]dt \tag{2.26}$$

2.3 Weibull Comparison

Each of these models has had some varying level of success when modeling the bathtub-shaped hazard function within their respective publications. Each of the modified Weibull models utilized the same reference data set with a known bathtub shaped hazard function from [26] shown in Table 2.2 which will be referred to as the Aarset Data Set throughout this paper.

Silva et. al showed in [22] that the BMW distribution was a better fit than the MW [21] and Additive Weibull [19] distributions while Almalki and Yuan showed that NMW is a better fit than BMW, so it follows that NMW is a better fit than BMW for the Aarset data set [26]. The Aarset [26] data set in Table 2.2 represents the lifetimes of 50 devices and contains no censored observations. Similarly, Sarhan & Apaloo [24] showed that EMWE fit the reference data better than the MW distribution.

Table 2.2: The Aarset Data Set

0.1	0.2	1	1	1	1	1	2	3	6
7	11	12	18	18	18	18	18	21	32
36	40	45	46	47	50	55	60	63	63
67	67	67	67	72	75	79	82	82	83
84	84	84	85	85	85	85	52	86	86

In 2013, J.K Freels [27] showed that the poly-Weibull distribution fit the same data set better than the NMW and EMWE distributions for the bi-Weibull and tri-Weibull. Some properties for the bi-Weibull and tri-Weibull will be developed from the raw moments and the poly-Weibull will be compared further with the NMW and EMWE distributions. The properties for the poly-Weibull will be determined using numerical methods and with a series expansion. A summary of the PDF's for these distributions is shown in Table 2.3.

Table 2.3: PDF for Weibull Distributions

Model	**PDF**
Weibull	$\frac{\beta}{\alpha}\left(\frac{t}{\alpha}\right)^{\beta-1}\exp\left[-\left(\frac{t}{\alpha}\right)^{\beta}\right]$
Additive Weibull	$\left(\frac{\beta_1}{\alpha_1}(\alpha_1 t)^{\beta_1-1}+\frac{\beta_2}{\alpha_2}(\alpha_2 t)^{\beta_2-1}\right)\exp\left[-(\alpha_1 t)^{\beta_1}-(\alpha_2 t)^{\beta_2}\right]$
Modified Weibull	$\lambda\beta\left(\frac{t}{\alpha}\right)^{\beta-1}\exp\left[\left(\frac{t}{\alpha}\right)^{\beta}+\lambda\alpha\left(1-\exp\left[\left(\frac{t}{\alpha}\right)^{\beta}\right]\right)\right]$
Beta Modified Weibull	$B(t\|a,b)=\int_0^1 t^{a-1}(1-t)^{b-1}dt=\frac{\Gamma(a)\Gamma(b)}{\Gamma(a+b)}$ $\frac{\alpha t^{\beta-1}(\beta+\lambda t)\exp[\lambda t]}{B(a.b)}\left(1-\exp\left[-\alpha t^{\beta}\exp[\lambda t]\right]\right)^{a-1} exp\left[-b\alpha t^{\beta}\exp[\lambda t]\right]$
New Modified Weibull Distribution	$\left(\alpha_1\beta_1 t^{\beta_1-1}+\alpha_2(\beta_2+\lambda t)t^{\beta_2-1}\exp[-\lambda t]\right)\exp\left[-\alpha_1 t^{\beta_1}-\alpha_2 t^{\beta_2}\exp[\lambda t]\right]$
Exponentiated Modified Weibull	$\alpha_2\beta_1\beta_2\left(\frac{t}{\alpha_1}\right)^{\beta_1-1}\exp\left[\left(\frac{t}{\alpha_1}\right)^{\beta_1}+\alpha_1\alpha_2\left(1-\exp\left[\left(\frac{t}{\alpha_1}\right)^{\beta_1}\right]\right)\right]\left[1-\exp\left[\alpha_1\alpha_2\left(1-\exp\left[\left(\frac{t}{\alpha_1}\right)^{\beta_1}\right]\right)\right]^{\beta_2}\right]^{\beta_2-1}$
poly-Weibull	$\exp\left[-\sum_{j=1}^{J}\left(\frac{t}{\alpha_j}\right)^{\beta_j}\right]\left[\sum_{j=1}^{J}\frac{\beta_j t^{\beta_j-1}}{\alpha_j^{\beta_j}}\right]$

2.4 Closed-Form Derivation of poly-Weibull Moments

It is common practice to determine the moments for a distribution when it is presented. The literature on the poly-Weibull distribution is limited and to date the moments have not been derived for the poly-Weibull distribution. Several attempts were made to solve the integral and are shown below. Each of the derivations below was motivated by the attempt shown before. Recall, first, that the moments for a distribution are given by

$$E\left[t^k\right] = \int_0^\infty t^k f(t)dt.$$

In the first derivation the equation will be manipulated into a form of the exponential family to solve the expected value equation. This manipulation will occur in the PDF

$$f\left(t|\alpha_j,\beta_j\right) = \exp\left[-\sum_{j=1}^{J}\left(\frac{t}{\alpha_j}\right)^{\beta_j}\right]\left[\sum_{j=1}^{J}\frac{\beta_j t^{\beta_j-1}}{\alpha_j^{\beta_j}}\right]$$

by letting

$$g\left(t\right) = -\sum_{j=1}^{J}\left(\frac{t}{\alpha_j}\right)^{\beta_j}.$$

taking the derivative of $g(t)$ gives

$$g'\left(t\right) = -\sum_{j=1}^{J}\frac{\beta_j t^{\beta_j-1}}{\alpha_j^{\beta_j}}.$$

Substituting this expression into the poly-Weibull PDF allows it to be written as:

$$f\left(t|\alpha_j,\beta_j\right) = \exp\left[g\left(t\right)\right]\left(-g'\left(t\right)\right) = -\exp\left[g\left(t\right)\right]g'\left(t\right) = -\frac{d}{dt}\exp\left[g\left(t\right)\right].$$

Using this expression for the poly-Weibull PDF allows us to restate the moment equation as

$$E\left[t^k\right] = \int_0^\infty t^k \left(-\frac{d}{dt}\exp\left[-g\left(t\right)\right]\right) dt.$$

Let:

$$u = t^k \qquad \& \qquad dv = -\frac{d}{dt}\exp\left[g\left(t\right)\right] dt$$

Which becomes:

$$du = kt^{k-1}dt \qquad \& \qquad v = -\exp\left[g\left(t\right)\right]$$

Plugging into the uv-substitution equation, we get:

$$\left\{-t^k \exp\left[g\left(t\right)\right]\right\}_0^\infty + k\int_0^\infty t^{k-1}\exp\left[g\left(t\right)\right] dt$$

The left-hand side goes to zero when the limits are evaluated, leaving only the right-hand-side:

$$k\int_0^\infty t^{k-1}\exp\left[g\left(t\right)\right] dt$$

Plugging the expression for $g(t)$ back in:

$$k\int_0^\infty t^{k-1}\exp\left[-\sum_{j=1}^{J}\left(\frac{t}{\alpha_j}\right)^{\beta_j}\right] dt \tag{2.27}$$

From here, it can be seen that this integral will not simplify to a form allowing a closed-form solution. At most, numerical integration could be applied to Eq. 2.27 to estimate the moments. This resembles what could be a gamma function, but the summation inside the exponential term presents difficulty employing mathematic modification by adding 0 to the exponent of t^{k-1}, or raising t to a power of 1. The inability to manipulate the equation further is due to the β exponent inside the exponential term.

Any modification to t^k outside of the exponential term to obtain a gamma function would result in changing the integral entirely.

Another attempt at solving $E\left[t^k\right]$ will be shown below. In the last method, a summation outside of the exponential term may have led to the integral being in the form of a gamma function. In this attempt, the sum outside of the exponential term will not be removed using uv-substitution. Rather, the t^k associated with the expected value equation will be distributed to the summation outside of the exponential term and the equation will be modified from that point. To simplify the process, the bi-Weibull is examined by letting $J = 2$:

$$f\left(t|\alpha_1,\alpha_2,\beta_1,\beta_2\right) = \exp\left[-\left(\left(\frac{t}{\alpha_1}\right)^{\beta_1} + \left(\frac{t}{\alpha_2}\right)^{\beta_2}\right)\right]\left[\frac{\beta_1 t^{\beta_1-1}}{\alpha_1^{\beta_1}} + \frac{\beta_2 t^{\beta_2-1}}{\alpha_2^{\beta_2}}\right]$$

$$\begin{aligned} E\left[t^k\right] &= \int_0^\infty t^k f\left(t|\alpha_1,\alpha_2,\beta_1,\beta_2\right) dt \\ &= \int_0^\infty t^k \exp\left[-\left(\left(\frac{t}{\alpha_1}\right)^{\beta_1} + \left(\frac{t}{\alpha_2}\right)^{\beta_2}\right)\right]\left[\frac{\beta_1 t^{\beta_1-1}}{\alpha_1^{\beta_1}} + \frac{\beta_2 t^{\beta_2-1}}{\alpha_2^{\beta_2}}\right] dt \end{aligned}$$

First, the t^k was distributed to the non-exponential term resulting the right-hand side of the equation shown below

$$= \int_0^\infty \left[\frac{\beta_1 t^{\beta_1+k-1}}{\alpha_1^{\beta_1}} + \frac{\beta_2 t^{\beta_2+k-1}}{\alpha_2^{\beta_2}}\right] \exp\left[-\left(\left(\frac{t}{\alpha_1}\right)^{\beta_1} + \left(\frac{t}{\alpha_2}\right)^{\beta_2}\right)\right]$$

Next, the integral will be multiplied by $\frac{\alpha^{k-1}}{\alpha^{k-1}}$ to set the equation up in a similar form to the well-known gamma function:

$$= \int_0^\infty \left[\alpha_1^{k-1}\beta_1\left(\frac{t}{\alpha_1}\right)^{\beta_1+k-1} + \alpha_2^{k-1}\beta_2\left(\frac{t}{\alpha_2}\right)^{\beta_2+k-1}\right] \exp\left[-\left(\left(\frac{t}{\alpha_1}\right)^{\beta_1} + \left(\frac{t}{\alpha_2}\right)^{\beta_2}\right)\right] dt$$

Distributing $\left[\alpha_1^{k-1}\beta_1\left(\frac{t}{\alpha_1}\right)^{\beta_1+k-1} + \alpha_2^{k-1}\beta_2\left(\frac{t}{\alpha_2}\right)^{\beta_2+k-1}\right]$ to the exponential term renders:

$$= \int_0^\infty \left(\alpha_1^{k-1}\beta_1\left(\frac{t}{\alpha_1}\right)^{\beta_1+k-1}\right)\exp\left[-\left(\left(\frac{t}{\alpha_1}\right)^{\beta_1} + \left(\frac{t}{\alpha_2}\right)^{\beta_2}\right)\right]dt$$
$$+ \int_0^\infty \left(\alpha_2^{k-1}\beta_2\left(\frac{t}{\alpha_2}\right)^{\beta_2+k-1}\right)\exp\left[-\left(\left(\frac{t}{\alpha_1}\right)^{\beta_1} + \left(\frac{t}{\alpha_2}\right)^{\beta_2}\right)\right]dt$$

Pulling the constants out of the integrals:

$$= \alpha_1^{k-1}\beta_1 \int_0^\infty \left(\frac{t}{\alpha_1}\right)^{\beta_1+k-1} \exp\left[-\left(\left(\frac{t}{\alpha_1}\right)^{\beta_1} + \left(\frac{t}{\alpha_2}\right)^{\beta_2}\right)\right]dt$$
$$+ \alpha_2^{k-1}\beta_2 \int_0^\infty \left(\frac{t}{\alpha_2}\right)^{\beta_2+k-1} \exp\left[-\left(\left(\frac{t}{\alpha_1}\right)^{\beta_1} + \left(\frac{t}{\alpha_2}\right)^{\beta_2}\right)\right]dt$$

Separating the sum within the exponential into products of exponentials using the first law of exponents ($e^{\sum a_i} = \prod e^{a_i}$):

$$= \alpha_1^{k-1}\beta_1 \int_0^\infty \left(\frac{t}{\alpha_1}\right)^{\beta_1+k-1} \exp\left[-\left(\frac{t}{\alpha_1}\right)^{\beta_1}\right]\exp\left[-\left(\frac{t}{\alpha_2}\right)^{\beta_2}\right]dt$$
$$+ \alpha_2^{k-1}\beta_2 \int_0^\infty \left(\frac{t}{\alpha_2}\right)^{\beta_2+k-1} \exp\left[-\left(\frac{t}{\alpha_1}\right)^{\beta_1}\right]\exp\left[-\left(\frac{t}{\alpha_2}\right)^{\beta_2}\right]dt$$

Now, let $u = \left(\frac{t}{\alpha_1}\right)^{\beta_1}$ & $v = \left(\frac{t}{\alpha_2}\right)^{\beta_2}$ and take the derivative of each.

$$du = \frac{\beta_1 t^{\beta_1-1}}{\alpha_1^{\beta_1}}dt = \frac{\beta_1}{t}\left(\frac{t}{\alpha_1}\right)^{\beta_1} dt = \frac{\beta_1 u}{t}dt \rightarrow dt = \frac{t}{\beta_1 u}du$$
$$dv = \frac{\beta_2 t^{\beta_2-1}}{\alpha_2^{\beta_2}}dt = \frac{\beta_2}{t}\left(\frac{t}{\alpha_2}\right)^{\beta_2} dt = \frac{\beta_2 v}{t}dt \rightarrow dt = \frac{t}{\beta_2 v}dv$$

Now, dt is a first order differential equation for both u & v with t still in the expression. However, t can be determined from u & v as $t = \alpha_1 u^{1/\beta_1}$ & $t = \alpha_2 v^{1/\beta_2}$, respectively. From

this, dt can be determined for u and v as $\frac{\alpha_1 u^{1/\beta_1 - 1}}{\beta_1} du$ & $\frac{\alpha_2 v^{1/\beta_2 - 1}}{\beta_2} dv$, respectively. Now, u, v, & each respective dt can be plugged into the integral for $E\left[t^k\right]$. Like-terms are then combined and constants are pulled outside of the integral.

$$= \alpha_1^{k-1}\beta_1 \int_0^\infty u^{(k-1)/\beta_1} \exp[-u] \exp[-v] \left(\frac{\alpha_1 u^{1/\beta_1 - 1}}{\beta_1} du\right) + \alpha_2^{k-1}\beta_2 \int_0^\infty v^{(k-1)/\beta_2} \exp[-u] \exp[-v] \left(\frac{\alpha_2 v^{1/\beta_2 - 1}}{\beta_2} dv\right)$$

$$= \alpha_1^{k-1}\beta_1 \left(\frac{\alpha_1}{\beta_1}\right) \int_0^\infty u^{(k-1)/\beta_1 + 1/\beta_1 - 1} \exp[-u] \exp[-v]\, du + \alpha_2^{k-1}\beta_2 \left(\frac{\alpha_2}{\beta_2}\right) \int_0^\infty v^{(k-1)/\beta_2 + 1/\beta_2 - 1} \exp[-u] \exp[-v]\, dv$$

$$= \alpha_1^k \int_0^\infty u^{k/\beta_1 - 1} \exp[-u] \exp[-v]\, du + \alpha_2^k \int_0^\infty v^{k/\beta_2 - 1} \exp[-u] \exp[-v]\, dv$$

The gamma function is in the form $\Gamma(k) = \int_0^\infty t^{k-1} \exp[-t]\, dt$, which could not be obtained as a closed-form solution because of the two exponential terms. The u & v terms could be solved with respect to one another by relating t or dt but this still does not lead to a closed form solution unless $\beta_1 = \beta_2$; which is simply the two-parameter Weibull. To further determine if it could become a gamma function, the attempt was made to reverse-engineer the poly-Weibull distribution starting with the gamma function. If successful, it would meet in the middle and a closed-form solution would be obtained.

The two-parameter Weibull uses u-substitution when developing an equation to find the moments. This process will begin with an integral to the point where a u-substitution as been performed.

$$\Gamma(\beta) = \int_0^\infty u^{\beta-1} \exp[-u]\, du$$

$$\text{where } \; u = \left(\frac{t}{\alpha}\right)^\beta$$

Then, take the derivative of u and put the integral in terms of t:

$$du = \beta \left(\frac{t}{\alpha}\right)^{\beta-1}$$

The integral becomes:

$$\Gamma(\beta) = \int_0^\infty \left(\frac{t}{\alpha}\right)^{\beta(\beta-1)} \exp\left[-\left(\frac{t}{\alpha}\right)^{\beta}\right]\left(\beta\left(\frac{t}{\alpha}\right)^{\beta-1}\right) dt$$

$$= \beta \int_0^\infty \frac{t^{\beta^2-\beta} t^{\beta-1}}{\alpha^{\beta^2-\beta}\alpha^{\beta-1}} \exp\left[-\left(\frac{t}{\alpha}\right)^{\beta}\right] dt$$

$$= \beta \int_0^\infty \frac{t^{\beta^2-1}}{\alpha^{\beta^2-1}}$$

$$= \beta \int_0^\infty \left(\frac{t}{\alpha}\right)^{\beta^2-1} \exp\left[-\left(\frac{t}{\alpha}\right)^{\beta}\right] dt$$

Sum J gamma functions:

$$\Gamma(\beta_1) + \Gamma(\beta_2) + \ldots + \Gamma(\beta_J)$$

$$= \beta_1 \int_0^\infty \left(\frac{t}{\alpha_1}\right)^{\beta_1^2-1} \exp\left[-\left(\frac{t}{\alpha_1}\right)^{\beta_1}\right] dt$$

$$+ \beta_2 \int_0^\infty \left(\frac{t}{\alpha_2}\right)^{\beta_2^2-1} \exp\left[-\left(\frac{t}{\alpha_2}\right)^{\beta_2}\right] dt$$

$$+ \ldots + \beta_J \int_0^\infty \left(\frac{t}{\alpha_J}\right)^{\beta_J^2-1} \exp\left[-\left(\frac{t}{\alpha_J}\right)^{\beta_J}\right] dt$$

This becomes:

$$\sum_{j=1}^{J} \Gamma\left(\beta_j\right) = \sum_{j=1}^{J} \beta_j \int_0^\infty \left(\frac{t}{\alpha_j}\right)^{\beta_j^2-1} \exp\left[-\left(\frac{t}{\alpha_j}\right)^{\beta_j}\right] dt$$

$$\sum_{j=1}^{J} \Gamma\left(\beta_j + k\right) = \sum_{j=1}^{J} \beta_j \int_0^\infty \left(\frac{t}{\alpha_j}\right)^{\beta_j^2+k-1} \exp\left[-\left(\frac{t}{\alpha_j}\right)^{\beta_j}\right] dt$$

Again, the same conclusion is reached because of the summation inside the integral (in addition to the β_j^2 term attached to t). A product of integrals would need to be created inside the integral which eliminates the equality. The raw moments can also be determined using numerical methods with Eq. 2.27, in the form:

$$E\left[t^k\right] = k \int_0^\infty t^{k-1} \exp\left[-\sum_{j=1}^{J} \left(\frac{t}{\alpha_j}\right)^{\beta_j}\right] dt \tag{2.28}$$

From here, it can be concluded that a closed-form solution could not be obtained using traditional methods of manipulating the equation into a form of the exponential family, distributing t^k and algebraically modifying the contents of the integral, or reverse-engineering the poly-Weibull starting from the gamma function. Power series are often used in situations such as these to reach a closed-form solution to to an integral. The poly-Weibull contains a summation inside of the exponential term which leads to many of the methods mentioned failing. The power series related to exponential terms is the Taylor-Series expansion, therefore this method should be performed to determine an equation for the moments.

III. Methodology

Finding an expression for the moments of a distribution allows one to generate the mean, variance, skewness, and kurtosis for that given distribution. An expression for the kth moment may be found by evaluating the equation below for the appropriate value of k.

$$E\left[t^k\right] = \int_0^\infty t^k f(t)\, dt \tag{3.1}$$

$$\text{where } k \in \mathbb{Z}^+$$

Evaluating this integral for $k = 1, 2, 3, 4$, gives the first four moments which lead to common properties for a given distribution. Determining an equation for the moments of the poly-Weibull distribution is left to a Taylor-Series approximation since a closed form solution was not possible using the methods shown in section 2.4. The first part of this derivation utilizes the same uv-substitution method shown in during the attempt at finding a closed-form solution in Chapter 2. Recall, the PDF of the poly-Weibull distribution is expressed as:

$$f\left(t|\alpha_j, \beta_j\right) = \exp\left[-\sum_{j=1}^{J}\left(\frac{t}{\alpha_j}\right)^{\beta_j}\right]\left[\sum_{j=1}^{J}\frac{\beta_j t^{\beta_j - 1}}{\alpha_j^{\beta_j}}\right].$$

Substituting this PDF into the moment equation (Eq. 3.1) results in the following integral to be evaluated

$$E\left[t^k\right] = \int_0^\infty t^k f\left(t|\alpha_j, \beta_j\right) dt = \int_0^\infty t^k \exp\left[-\sum_{j=1}^{J}\left(\frac{t}{\alpha_j}\right)^{\beta_j}\right]\left[\sum_{j=1}^{J}\frac{\beta_j t^{\beta_j - 1}}{\alpha_j^{\beta_j}}\right] dt.$$

The lower bound of this moment equation is 0 since the poly-Weibull is defined overthe support region $[0, \infty)$. The derivation for the moments, using the Taylor-series approximation, will be shown for the bi-Weibull distribution, the tri-Weibull distribution

equation is given at the end with the derivation show in Appendix A.4. We start with setting up the bi-Weibull distributions by setting $J = 2$:

$$f\left(t|\alpha_1,\alpha_2,\beta_1,\beta_2\right) = \exp\left[-\left(\frac{t}{\alpha_1}\right)^{\beta_1} - \left(\frac{t}{\alpha_2}\right)^{\beta_2}\right]\left[\frac{\beta_1 t^{\beta_1-1}}{\alpha_1^{\beta_1}} + \frac{\beta_2 t^{\beta_2-1}}{\alpha_2^{\beta_2}}\right]$$

3.1 Derivation of bi-Weibull Moments

Setting up the moment equation:

$$\begin{aligned} E\left[t^k\right] &= \int_0^\infty t^k f\left(t|\alpha_1,\alpha_2,\beta_1,\beta_2\right) dt \\ &= \int_0^\infty t^k \exp\left[-\left(\frac{t}{\alpha_1}\right)^{\beta_1} - \left(\frac{t}{\alpha_2}\right)^{\beta_2}\right]\left[\frac{\beta_1 t^{\beta_1-1}}{\alpha_1^{\beta_1}} + \frac{\beta_2 t^{\beta_2-1}}{\alpha_2^{\beta_2}}\right] dt \end{aligned}$$

Since it is known that the PDF is the derivative of the CDF (Eq. 1.4), the PDF $f\left(t|\alpha_1,\alpha_2,\beta_1,\beta_2\right)$ can be rewitten as the negative derivative of the exponential term:

$$\exp\left[-\left(\frac{t}{\alpha_1}\right)^{\beta_1} - \left(\frac{t}{\alpha_2}\right)^{\beta_2}\right]\left[\frac{\beta_1 t^{\beta_1-1}}{\alpha_1^{\beta_1}} + \frac{\beta_2 t^{\beta_2-1}}{\alpha_2^{\beta_2}}\right] = -\frac{d}{dt}\exp\left[-\left(\frac{t}{\alpha_1}\right)^{\beta_1} - \left(\frac{t}{\alpha_2}\right)^{\beta_2}\right]$$

This allows the integral to be simplified as

$$\rightarrow \int_0^\infty t^k\left(-\frac{d}{dt}\exp\left[-\left(\frac{t}{\alpha_1}\right)^{\beta_1} - \left(\frac{t}{\alpha_2}\right)^{\beta_2}\right]\right) dt.$$

Next, terms are assigned to u and dv and the derivative of u and anti-derivative of dv are determined. These values are

$$u = t^k \qquad dv = -\frac{d}{dt}\exp\left[-\left(\frac{t}{\alpha_1}\right)^{\beta_1} - \left(\frac{t}{\alpha_2}\right)^{\beta_2}\right] dt$$

$$du = kt^{k-1}dt \qquad v = -\exp\left[-\left(\frac{t}{\alpha_1}\right)^{\beta_1} - \left(\frac{t}{\alpha_2}\right)^{\beta_2}\right]$$

substituting these values into $uv - \int vdu$ gives the following expression

$$= \left\{ -t^k \exp\left[-\left(\frac{t}{\alpha_1}\right)^{\beta_1} - \left(\frac{t}{\alpha_2}\right)^{\beta_2} \right] \right\}_0^\infty + \int_0^\infty kt^{k-1} \exp\left[-\left(\frac{t}{\alpha_1}\right)^{\beta_1} - \left(\frac{t}{\alpha_2}\right)^{\beta_2} \right] dt.$$

As was shown in Section 2.4, the left-hand-side of this equation goes to 0 and only the right-hand-side remains to be solved

$$= k \int_0^\infty t^{k-1} \exp\left[-\left(\frac{t}{\alpha_1}\right)^{\beta_1} - \left(\frac{t}{\alpha_2}\right)^{\beta_2} \right] dt.$$

Since it is known that $e^{\sum a_i} = \prod e^{a_i}$, the exponents may broken up as follows

$$= k \int_0^\infty t^{k-1} \exp\left[-\left(\frac{t}{\alpha_1}\right)^{\beta_1} \right] \exp\left[-\left(\frac{t}{\alpha_2}\right)^{\beta_2} \right] dt.$$

The Taylor-series expansion is now applied to the second exponential term, as the first exponential term is retained to eventually build towards a gamma function as is done to determine the moments of the two-parameter Weibull distribution

$$= k \int_0^\infty t^{k-1} \exp\left[-\left(\frac{t}{\alpha_1}\right)^{\beta_1} \right] \sum_{n=0}^{\infty} \frac{\left(-\left(\frac{t}{\alpha_2}\right)^{\beta_2} \right)^n}{n!} dt.$$

The next steps involve algebraic manipulation of the equation to obtain a form that resembles the gamma function, $\Gamma(\beta) = \int_0^\infty t^{\beta-1} \exp[-t]\, dt$

$$= k \int_0^\infty t^{k-1} \exp\left[-\left(\frac{t}{\alpha_1}\right)^{\beta_1} \right] \sum_{n=0}^{\infty} \frac{\left(-\frac{t^{\beta_2}}{\alpha_2^{\beta_2}} \right)^n}{n!} dt. \tag{3.2}$$

The summation and terms not attached to the time variable t are now pulled out of the integral using termwise integration (Eq. A.5 in Appendix A.1) followed by combining the t terms. Series expansion is known to be absolutely convergent [28], but termwise integration requires that the function inside the sum must be uniformly convergent.

3.1.1 Uniform Convergence Proof.

The integral shown in Eq. 3.2 goes to infinity while the definition for termwise integration is over some compact region. However, it is known that $\exists T > t$ in many situations, therefore the integral is not always infinite and termwise integration can be applied. Recall first that the integral being evaluated is given in Eq. A.1:

$$E\left(t^k\right) = \int_0^\infty t^k f(t)dt$$

Using Eqs: 1.1, 1.2, & 1.4:

$$f(t) = \frac{d}{dt}F(t)$$

$$F(t) = 1 - R(t)$$

$$\rightarrow f(t) = \frac{d}{dt}(1 - R(t)) = -\frac{d}{dt}R(t)$$

$$\rightarrow -\int_0^\infty t^k \frac{d}{dt}R(t)dt$$

$$R(t) = Pr(T > t) \ni T \geq 0$$

$$\therefore \exists T > t$$

There are cases, such as right-censored data, where the t would have to be assumed to be infinite. Therefore, this may not always be true. However, since we never carry test out to infinity we can assume this to be true.

A series with sum $s(z)$ is called uniformly convergent in a region G if $\forall\ \epsilon > 0$ we can find a $N = N(\epsilon)$, not depending on $z \ni |s_n(z) - s(z)| < \epsilon\ \forall n > N$ and $\forall z \in G$ [28]. Here, t, m, and M will be used in place of z, n, and N, respectively. Suppose $t \in G$ and $\exists\ \epsilon > 0$. Also, suppose $\exists(a, b) \in G \in \mathbb{R}^+$ where $M = max\{|a|, |b|\}$. Per the definition, $s(t)$ is defined as:

$$s(t) = \sum_{n=0}^{\infty} \frac{\left(-\frac{t^{\beta_2}}{\alpha_2^{\beta_2}}\right)^n}{n!}$$

The mth term is given by:

$$s_m(t) = \sum_{n=0}^{m} \frac{\left(-\frac{t^{\beta_2}}{\alpha_2^{\beta_2}}\right)^n}{n!}$$

Therefore:

$$\begin{aligned}
|s_m(t) - s(t)| &= \left| \sum_{n=0}^{m} \frac{\left(-\frac{t^{\beta_2}}{\alpha_2^{\beta_2}}\right)^n}{n!} - \sum_{n=0}^{\infty} \frac{\left(-\frac{t^{\beta_2}}{\alpha_2^{\beta_2}}\right)^n}{n!} \right| \\
&= \left| -\sum_{n=m+1}^{\infty} \frac{\left(-\frac{t^{\beta_2}}{\alpha_2^{\beta_2}}\right)^n}{n!} \right| \\
&= \left| \sum_{n=m+1}^{\infty} \frac{\left(-\frac{t^{\beta_2}}{\alpha_2^{\beta_2}}\right)^n}{n!} \right|
\end{aligned}$$

If $\exists M \in G \in \mathbb{R}^+ \ni m > M$ and $\left|\left(-\frac{t^{\beta_2}}{\alpha_2^{\beta_2}}\right)\right| < M$, then:

$$\begin{aligned}
|s_m(t) - s(t)| &= \left| \sum_{n=m+1}^{\infty} \frac{\left(-\frac{t^{\beta_2}}{\alpha_2^{\beta_2}}\right)^n}{n!} \right| \\
&\leq \left| \sum_{n=m+1}^{\infty} \frac{M^n}{n!} \right|
\end{aligned}$$

As $m \to \infty$, $n \to \infty$ as well, and

$$\sum_{n=m+1}^{\infty} \frac{M^n}{n!} \to 0$$

$$\therefore |s_m(t) - s(t)| = \left| \sum_{n=0}^{m} \frac{\left(-\frac{t^{\beta_2}}{\alpha_2^{\beta_2}}\right)^n}{n!} - \sum_{n=0}^{\infty} \frac{\left(-\frac{t^{\beta_2}}{\alpha_2^{\beta_2}}\right)^n}{n!} \right| = \left| \sum_{n=m+1}^{\infty} \frac{\left(-\frac{t^{\beta_2}}{\alpha_2^{\beta_2}}\right)^n}{n!} \right| \leq \left| \sum_{n=m+1}^{\infty} \frac{M^n}{n!} \right| = 0 < \epsilon \quad \square$$

This proof is for a closed region, G, and the integral in which termwise integration is being applied to, is infinite. There may exists situations where this would not hold as true and the derived equation cannot be used. It has been shown that the series is uniformly convergent over some closed region and uniform convergence will be assumed to be true for this derivation. The above proof will serve as a basis for stating this as a proposition for the infinite integral. Therefore, termwise integration will be applied and the integral shall be moved within the summation resulting in the following expression:

$$E\left[t^k\right] = k\sum_{n=0}^{\infty} \frac{1}{\left(-\alpha_2^{\beta_2}\right)^n n!} \int_0^{\infty} t^{k-1} \exp\left[-\left(\frac{t}{\alpha_1}\right)^{\beta_1}\right] t^{n\beta_2} dt.$$

Rearranging terms involving t then gives the following expression

$$E\left[t^k\right] = k\sum_{n=0}^{\infty} \frac{1}{\left(-\alpha_2^{\beta_2}\right)^n n!} \int_0^{\infty} t^{k+n\beta_2-1} \exp\left[-\left(\frac{t}{\alpha_1}\right)^{\beta_1}\right] dt$$

Next, define the substitution of the term inside of the exponent $u = \left(\frac{t}{\alpha_1}\right)^{\beta_1}$ and take the derivative to obtain du

$$du = \frac{\beta_1 t^{\beta_1-1}}{\alpha_1^{\beta_1}} dt = \frac{\beta_1 t^{\beta_1}}{\alpha_1^{\beta_1} t} dt.$$

Using this expression, we solve for dt and plug the result into the integral along with u. The t^{-1} cancels with the t in $t^{k+n\beta_2-1}$. This gives the following result

$$\begin{aligned}
dt &= \frac{\alpha_1^{\beta_1} t}{\beta_1 t^{\beta_1}} du = \frac{t}{\beta_1}\left(\frac{\alpha_1^{\beta_1}}{t^{\beta_1}}\right) du = \frac{t}{\beta_1}\left(\frac{\alpha_1}{t}\right)^{\beta_1} du = \frac{t}{u\beta_1} du \\
\rightarrow &= k\sum_{n=0}^{\infty} \frac{1}{\left(-\alpha_2^{\beta_2}\right)^n n!} \int_0^{\infty} t^{k+n\beta_2-1} \exp\left[-u\right] \left(\frac{t}{u\beta_1} du\right) \\
&= \frac{k}{\beta_1}\sum_{n=0}^{\infty} \frac{1}{\left(-\alpha_2^{\beta_2}\right)^n n!} \int_0^{\infty} t^{k+n\beta_2} \exp\left[-u\right] u^{-1} du.
\end{aligned}$$

Rearranging $u = \left(\frac{t}{\alpha_1}\right)^{\beta_1}$, renders the following expression

$$\rightarrow \alpha_1 u^{1/\beta_1} = t$$

which is plugged into the integral for t. The α_1 term is pulled out of the integral and u^{-1} is combined with $u^{(k+n\beta_2)/\beta_1}$ giving

$$\begin{aligned}
&= \frac{k}{\beta_1}\sum_{n=0}^{\infty}\frac{1}{\left(-\alpha_2^{\beta_2}\right)^n n!}\int_0^{\infty}\left(\alpha_1 u^{1/\beta_1}\right)^{k+n\beta_2}\exp\left[-u\right]u^{-1}du \\
&= \frac{k}{\beta_1}\sum_{n=0}^{\infty}\frac{\alpha_1^{k+n\beta_2}}{\left(-\alpha_2^{\beta_2}\right)^n n!}\int_0^{\infty}u^{(k+n\beta_2)/\beta_1}\exp\left[-u\right]u^{-1}du \\
&= \frac{k}{\beta_1}\sum_{n=0}^{\infty}\frac{\alpha_1^{k+n\beta_2}}{\left(-\alpha_2^{\beta_2}\right)^n n!}\int_0^{\infty}u^{\frac{k+n\beta_2}{\beta_1}-1}\exp\left[-u\right]du
\end{aligned}$$

which results in an integral expression in the form of the gamma function for u

$$= \frac{k}{\beta_1}\sum_{n=0}^{\infty}\frac{\alpha_1^{k+n\beta_2}}{\left(-\alpha_2^{\beta_2}\right)^n n!}\Gamma\left(\frac{k+n\beta_2}{\beta_1}\right). \tag{3.3}$$

The derivation is complete and Eq. 3.3 is the expected value equation for the bi-Weibull distribution. At this point, this equation can be used to determine the raw moments which results in statistical properties such as the mean, variance, skewness, and kurtosis.

For the tri-Weibull ($J = 3$), the process is the same with the β_1 term still left inside the integral and Taylor-Series expansion applied to the exponential term containing β_3 in addition to the exponential term containing β_2. Both sums are pulled outside of the integral just as the authors did in [23] to obtain an expected value equation for the NMW distribution. Once the sums are pulled outside the integral, the remaining steps in turning the integral into a gamma function are identical. The tri-Weibull derivation is shown in Appendix A.4 resulting in Eq. 3.4.

$$= \frac{k}{\beta_1} \sum_{n_1=0}^{\infty} \sum_{n_2=0}^{\infty} \frac{\alpha_1^{k+n_1\beta_2+n_2\beta_3}}{\left(-\alpha_2^{\beta_2}\right)^{n_1} \left(-\alpha_3^{\beta_3}\right)^{n_2} n_1! n_2!} \Gamma\left(\frac{k + n_1\beta_2 + n_2\beta_3}{\beta_1}\right) \tag{3.4}$$

The expected value equations shown in Eq. 3.3 & Eq. 3.4 reveals an expected pattern for the poly-Weibull; the number of infinite-summations and distributed β and n terms is $j-1$. The product of sums can then be represented as $\prod \sum$ starting with $j = 2$ for the product operator and $n_{j-1} = 0$ for the summation operator. The gamma function contains another infinite sum starting from $j = 2$ where n_{j-1} is multiplied by β_j. Although J.K. Freels [27] has shown that the bi-Weibull and tri-Weibull are as far as one needs to go, if someone was to find it necessary to examine a quad-Weibull distribution they would easily be able to determine the moment estimation using Eq. 3.5 shown below.

$$E_J\left[t^k\right] = \frac{\alpha_1^k k}{\beta_1} \left[\prod_{j=2}^{J} \sum_{n_{j-1}=0}^{\infty} \frac{\alpha_1^{n_{j-1}\beta_j}}{\left(-\alpha_j^{\beta_j}\right)^{n_{j-1}} n_{j-1}!}\right] \times \Gamma\left(\frac{k + \sum_j^J n_{j-1}\beta_j}{\beta_1}\right) \tag{3.5}$$

where $J, k \in \mathbb{Z}^+$

IV. Results

The moment equations derived in the previous chapter are used here to determine several summary measures, namely the mean, variance, skewness, and kurtosis for the bi-Weibull and tri-Weibull distributions. These summary measures are functions of one or more of the first four raw moments, which can be computed by setting $k = 1, 2, 3, 4$ in Equations 3.3 and 3.4. The expressions for these raw moments are shown in Table 4.1.

Table 4.1: First 4 raw moments for bi-Weibull & tri-Weibull

k	**bi-Weibull** $E_2\left[t^k\right]$	**tri-Weibull** $E_3\left[t^k\right]$
1	$\frac{\alpha_1}{\beta_1}\sum_{n=0}^{\infty}\frac{\alpha_1^{n\beta_2}}{\left(-\alpha_2^{\beta_2}\right)^n n!}\Gamma\left(\frac{1+n\beta_2}{\beta_1}\right)$	$\frac{\alpha_1}{\beta_1}\sum_{n_1=0}^{\infty}\sum_{n_2=0}^{\infty}\frac{\alpha_1^{n_1\beta_2+n_2\beta_3}}{\left(-\alpha_2^{\beta_2}\right)^{n_1}\left(-\alpha_3^{\beta_3}\right)^{n_2} n_1!n_2!}\Gamma\left(\frac{1+n_1\beta_2+n_2\beta_3}{\beta_1}\right)$
2	$\frac{2\alpha_1^2}{\beta_1}\sum_{n=0}^{\infty}\frac{\alpha_1^{n\beta_2}}{\left(-\alpha_2^{\beta_2}\right)^n n!}\Gamma\left(\frac{2+n\beta_2}{\beta_1}\right)$	$\frac{2\alpha_1^2}{\beta_1}\sum_{n_1=0}^{\infty}\sum_{n_2=0}^{\infty}\frac{\alpha_1^{n_1\beta_2+n_2\beta_3}}{\left(-\alpha_2^{\beta_2}\right)^{n_1}\left(-\alpha_3^{\beta_3}\right)^{n_2} n_1!n_2!}\Gamma\left(\frac{2+n_1\beta_2+n_2\beta_3}{\beta_1}\right)$
3	$\frac{3\alpha_1^3}{\beta_1}\sum_{n=0}^{\infty}\frac{\alpha_1^{n\beta_2}}{\left(-\alpha_2^{\beta_2}\right)^n n!}\Gamma\left(\frac{3+n\beta_2}{\beta_1}\right)$	$\frac{3\alpha_1^3}{\beta_1}\sum_{n_1=0}^{\infty}\sum_{n_2=0}^{\infty}\frac{\alpha_1^{n_1\beta_2+n_2\beta_3}}{\left(-\alpha_2^{\beta_2}\right)^{n_1}\left(-\alpha_3^{\beta_3}\right)^{n_2} n_1!n_2!}\Gamma\left(\frac{3+n_1\beta_2+n_2\beta_3}{\beta_1}\right)$
4	$\frac{4\alpha_1^4}{\beta_1}\sum_{n=0}^{\infty}\frac{\alpha_1^{n\beta_2}}{\left(-\alpha_2^{\beta_2}\right)^n n!}\Gamma\left(\frac{4+n\beta_2}{\beta_1}\right)$	$\frac{4\alpha_1^4}{\beta_1}\sum_{n_1=0}^{\infty}\sum_{n_2=0}^{\infty}\frac{\alpha_1^{n_1\beta_2+n_2\beta_3}}{\left(-\alpha_2^{\beta_2}\right)^{n_1}\left(-\alpha_3^{\beta_3}\right)^{n_2} n_1!n_2!}\Gamma\left(\frac{4+n_1\beta_2+n_2\beta_3}{\beta_1}\right)$

For a random variable T the mean is the first raw moment of the expected value of a distribution and is often denoted as

$$\mu = E[T].$$

The variance $\mathrm{Var}(T)$ is the second central moment for random variable T. Variance is often denoted by σ^2 and is a function of the first and second raw moments where

$$Var[T] = \sigma^2 = E[T^2] - (E[T])^2 .$$

Skewness is the third standardized moment of the random variable T. The skewness value is a measure of the asymmetry of the distribution about its mean and can be positive, negative, or undefined. Skewness can be determined by dividing the third centralized moment by σ^3 and is expressed as

$$Sk[T] = \frac{E[T^3] - 3\mu \text{ Var}[T] - \mu^3}{\sigma^3}.$$

Finally, the kurtosis is the fourth standardized moment of the random variable T. The kurtosis value is a measure of the "tailedness" of the distribution and can be determined by dividing the fourth central moments by σ^4. Kurtosis is often denoted by the symbol κ and is expressed as

$$\kappa[T] = \frac{E[T^4] - 4\mu E[T^3] + 6\mu^2 E[T^2] - 3\mu^4}{\sigma^4}.$$

These four statistical properties are shown in more detail with respect to the raw and centralized moments in Appendix A.3. Identifiability is important for the use of Eq. 3.5, meaning different values of the parameters will generate different probability distributions of the observable variables. By definition, this means that if we let $\mathcal{P} = \{P_\theta | \theta \in \Theta\}$ be a statistical model where the parameter space Θ is either finite- or infinite-dimensional; $\mathcal{P}$ is identifiable if the mapping $\theta \mapsto P_\theta$ is one-to-one, ie: $P_{\theta_m} = P_{\theta_n} \iff \theta_m = \theta_n$. It should be noted that for both the bi-Weibull and tri-Weibull that the identification conditions are such that the $\beta < 1$ value cannot be β_1. For simplification, the additional requirement that $\beta_1 > \beta_2 > \beta_3$ will be implemented.

4.1 Statistical Properties of poly-Weibull moments

The Aarset [26] dataset shown in Table 2.2 has a known bathtub shaped hazard function. This dataset has often been used to compare the performance of various distributions that have been developed for modeling data known to produce a bathtub shaped hazard function. Keeping with the trend of utilizing this data set to examine modified Weibull distributions, the α_j & β_j parameters are determined from this data set and will be used to test the statistical properties derived from Eq. 3.5. Solving a system of non-linear equations from the log-likelihood function cannot be accomplished analytically and Newtonian or quasi-Newtonian numerical optimization techniques can be tedious as finding a solution is highly sensitive on the starting values for the parameters in each equation. It would be simpler to obtain accurate parameter estimates by maximizing the log-likelihood function directly using a quasi-Newtonian algorithm. However, for asymptotic interval estimation, the optimization algorithm can produce inaccurate Hessian matrices leading to negative values along the diagonal of the covariance matrix. Thus, for finding the standard errors of the poly-Weibull model parameters the components of the observed Fisher information matrix have been derived analytically by J.K. Freels [27]. Using this method led to the the α_j & β_j parameter values for the bi-Weibull and tri-Weibull distributions shown in Table 4.2.

Table 4.2: bi-Weibull & tri-Weibull MLE's for the Aarset Data Set

bi-Weibull:	$\alpha_1 = 84.907$	$\alpha_2 = 61.663$		$\beta_1 = 82.334$	$\beta_2 = 0.702$	
tri-Weibull:	$\alpha_1 = 85.091$	$\alpha_2 = 92.299$	$\alpha_3 = 122.478$	$\beta_1 = 98.152$	$\beta_2 = 4.215$	$\beta_2 = 0.524$

From here, the mean, variance, standard deviation, skewness, and kurtosis can be determined for the bi-Weibull and tri-Weibull. The summations will be carried out to a level of tolerance of 1×10^{-4}. The tolerance was varied from 1×10^{-4} to 1×10^{-1}. At 1×10^{-1}, the number of iterations of the sum was only reduced by 5; the mean value was only different by 0.0015. Each of the remaining statistical properties were not significantly changed, either. At certain levels of tolerance, the higher moments would reach the tolerance in 1 less iteration. For this data set, the computational cost for each tolerance was minimal and the number of iterations for each moment was the same at a tolerance of 1×10^{-4}, therefore that level of tolerance was selected. These calculations were completed using the α & β values shown in Table 4.2 for bi-Weibull & tri-Weibull. These values were obtained from the Aarset [26] data set (Table 2.2).

4.1.1 Mean & Standard Deviation.

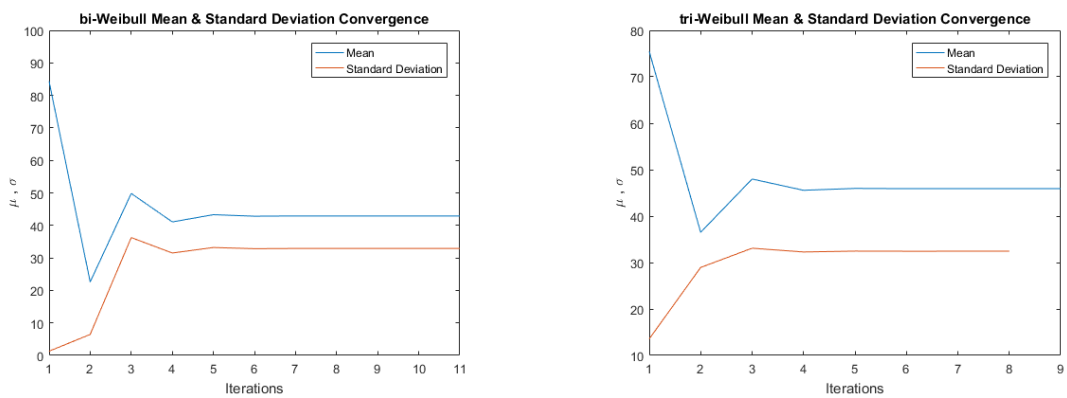

(a) bi-Weibull Mean & Standard Deviation

(b) tri-Weibull Mean & Standard Deviation Outer Sum

Figure 4.1: Convergence of bi-Weibull & tri-Weibull Mean & Standard Deviation

Using the code shown in Appendices B.1.1 & B.1.2 with the ML parameter estimates listed in Table 4.2, the bi-Weibull & tri-Weibull mean and standard deviation were

determined. Figure 4.1a shows the mean and standard deviation converge to an acceptable value after only 11 iterations for the bi-Weibull. Figure 4.1b shows the outer sum for the mean and standard deviation. The mean converges after 9 iterations while the standard deviation converges after only 8 iterations. The figures show little movement after the interations 4 and 5 because the tolerance level changes are on the order of $10^{-}4$.

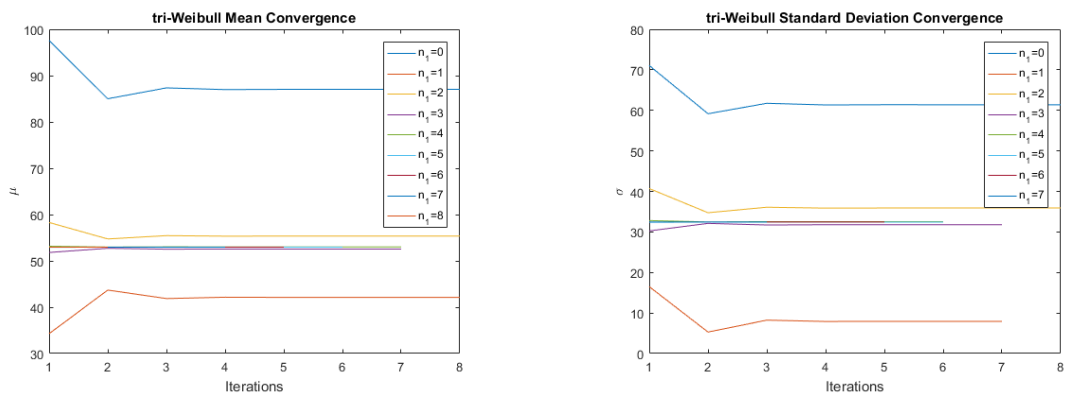

(a) Mean

(b) Standard Deviation

Figure 4.2: Convergence of tri-Weibull Mean & Standard Deviation Inner Sum

The tri-Weibull moment equation consists of 2 summation terms. The first summation term (inner sum) for the mean and standard deviation is shown in Figure 4.2. The two outermost lines with respect to the y-axis ($n_1 = 0$ and $n_1 = 1$) are the first two runs of the inner sum and show that the mean and standard deviation begin to converge by $n_1 = 2$. The values begin to converge as the lines get closer to one another and each line begins to require less iterations to reach the specified tolerance by $n_2 = 3$. The final churn of the inner sum for the mean ($n_1 = 8$) only runs for two iterations while the variance ($n_1 = 7$) only runs for three iterations.

4.1.2 Variance.

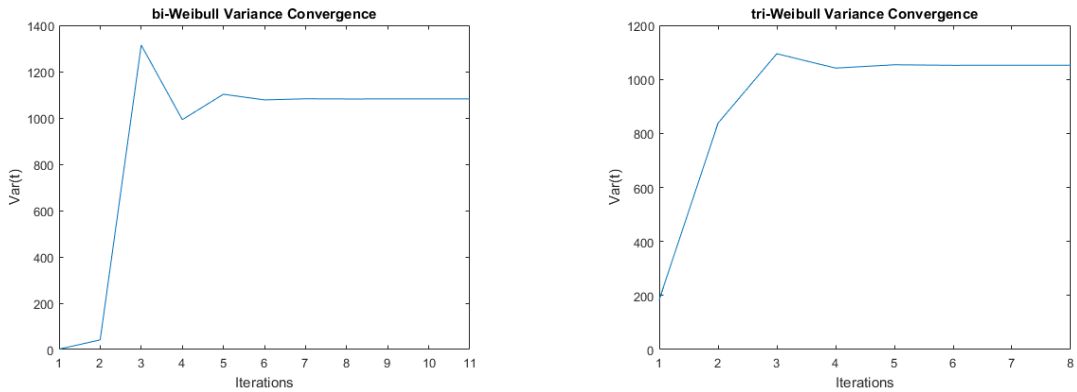

(a) bi-Weibull Variance

(b) tri-Weibull Variance Outer Sum

Figure 4.3: Convergence of bi-Weibull & tri-Weibull Outer Variance

Figure 4.3 shows the convergence of variance for the bi-Weibull and tri-Weibull distributions. The standard deviation shown above resulted from the variance values obtained so the activity is similar. For the bi-Weibull distribution, the variance converged after 11 iterations while the tri-Weibull outer sum converged in 8 iterations. Both plots in Figure 4.3 show less activity after $n = 5$ based on the dimensions of the plot which was close to the cutoff when the tolerance was examined at 10^{-1}. The inner sum of the variance for the tri-Weibull is shown in Figure 4.4. The activity is the same as that of the standard deviation; by $n_1 = 2$ the lines move closer together and by $n_1 = 3$ the lines become shorter.

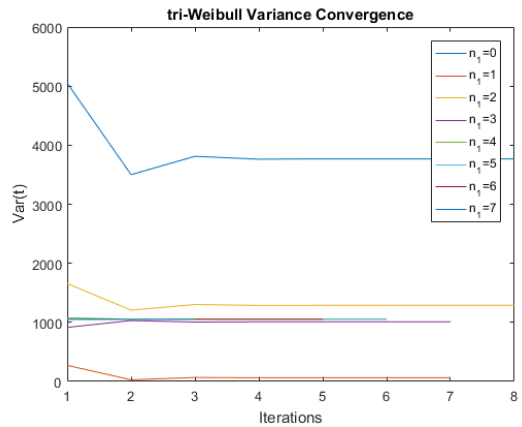

Figure 4.4: tri-Weibull Variance Inner Sum

4.1.3 Skewness.

Skewness is a measure of the symmetry of the shape of a distribution. A positive skewness value indicates that the distribution is positively skewed or right-tailed. Alternatively a negative skewness value indicates that the distribution is negatively skewed or left-tailed. A skewness value of zero indicates that the distribution is symmetric.

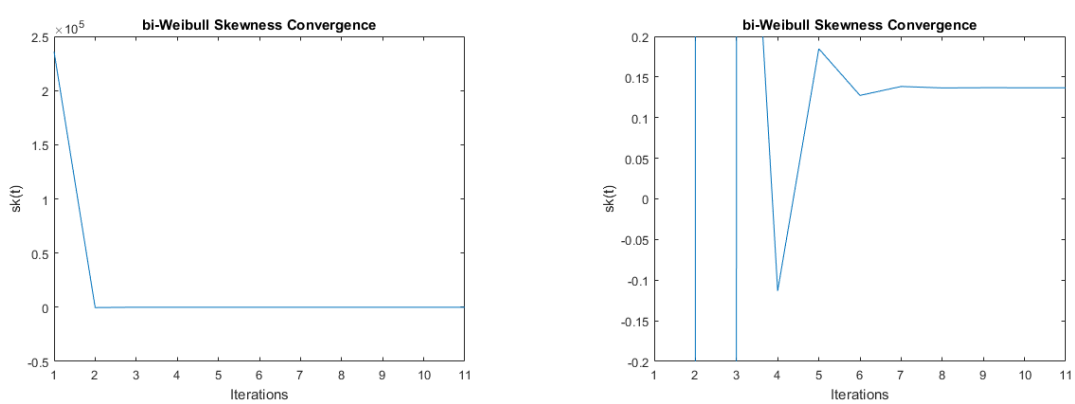

(a) Standard Plot

(b) Zoomed In

Figure 4.5: Convergence of bi-Weibull Skewness

Figure 4.5a shows very little change in the skewness value after 2 iterations. However, zooming in on the elbow of this curve, as shown in Figure 4.5b, reveals that the activity begins to slow even at the micro level after 7 iterations.

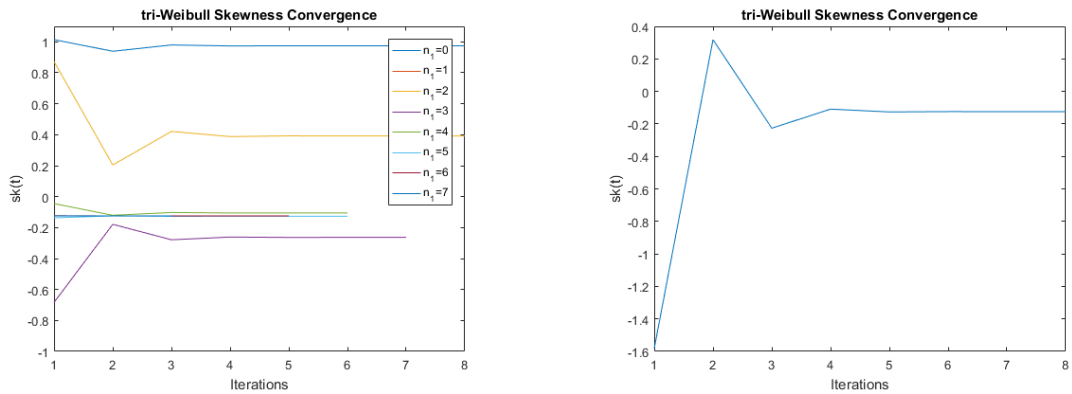

(a) Inner Sum

(b) Outer Sum

Figure 4.6: Convergence of tri-Weibull Inner & Outer Sum Skewness

The inner sum for the tri-Weibull skewness (Figure 4.6a) shows little activity after $n_2 = 4$. The two outermost lines are the first two runs when $n_1 = 1, 2$; once $n_1 > 1$ the lines begin to converge on themselves. Just as with the variance, the lines get shorter when $n_2 > 2$; when $n_2 = 7$, the inner sum only churns through 3 iterations. Figure 4.6b shows the outer sum for the skewness. It can be seen that the skewness converges to a value after $n_1 = 4$ at a tolerance of 1×10^{-2}; the remaining 4 iterations are changes to the ten-thousandths place.

4.1.4 Kurtosis.

Kurtosis measures the distributions flatness or peakedness. A distribution is referred to as platykurtic, or leptokurtic if it appears flat or peaked, respectively.

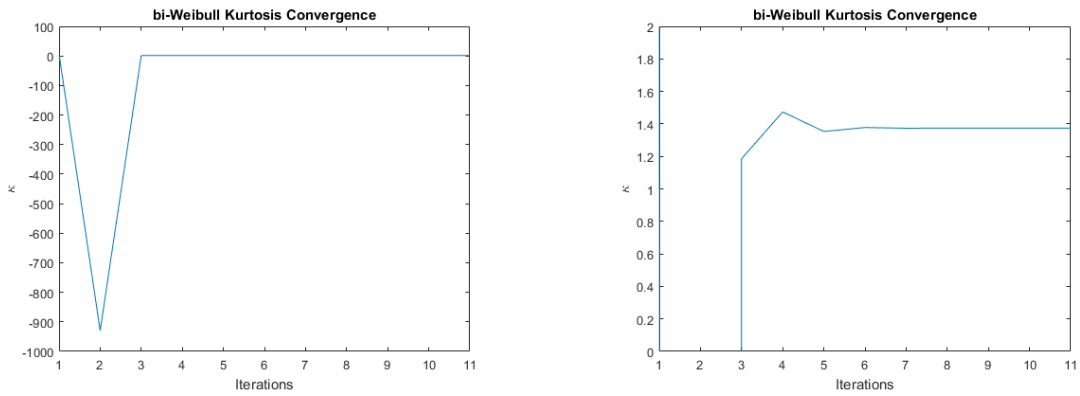

(a) Standard Plot

(b) Zoomed In

Figure 4.7: Convergence of bi-Weibull Kurtosis

Kurtosis showed similar behavior as skewness for the bi-Weibull seeming like it converges after only three iterations (Figure 4.7a). When zoomed in further in Figure 4.7b, the changes are minimal after 6 iterations. However, these changes are only shown at to the $10^{-}1$ level in the zoomed plot. The inner sum for the kurtosis shown in Figure 4.7b shows similar activity to the skewness.

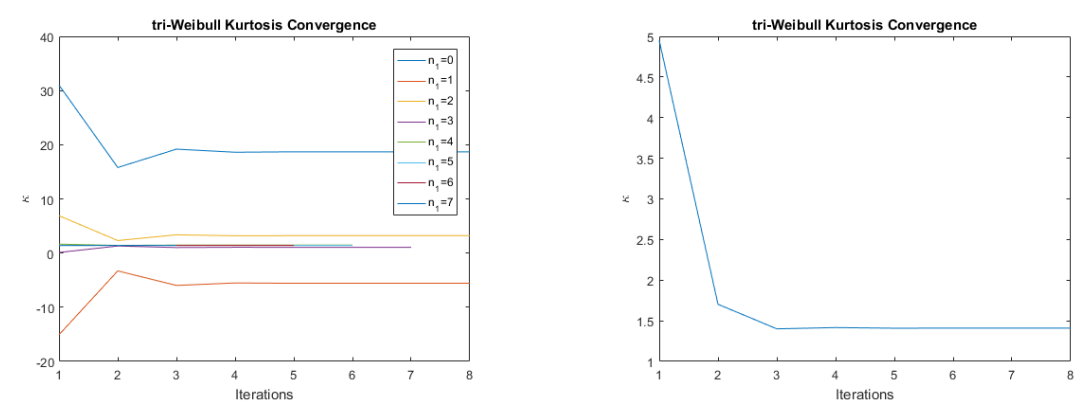

(a) Inner Sum

(b) Outer Sum

Figure 4.8: Convergence of tri-Weibull Inner & Outer Sum Kurtosis

Figure 4.8 shows the inner and outer sum for the kurtosis of the tri-Weibull. The activity shown in Figure 4.8a resembles the same behavior as each of the other tri-Weibull statistical properties for the inner sum. The final churn ($n_1 = 7$) of the inner sum for the kurtosis runs for only 3 iterations. The changes were minimal on the 10^{-1} scale shown in the plots after $n_1 = 3$ for the kurtosis.

4.1.5 Obtained Values.

Table 4.3 shows the values for the mean, variance, standard deviation, skewness, and kurtosis obtained for the bi-Weibull and tri-Weibull using Eqs. 3.3 & 3.4, respectively.

Table 4.3: tri-Weibull Mean, Variance, & Standard Deviation

	bi-Weibull	**tri-Weibull**
μ	42.8995	45.9151
σ	32.8929	32.4370
Var[T]	1081.9429	1052.1619
$Sk[T]$	0.1368	−0.1246
$\kappa[T]$	1.3739	1.4095

The values for the bi-Weibull and tri-Weibull are mostly similar. The tri-Weibull has a higher mean but lower variance; leading to a slightly smaller standard deviation. Based on the values obtained, the kurtosis indicates the the bi-Weibull and tri-Weibull are both platykurtic with values less than three. The skewness for the bi-Weibull and tri-Weibull are interesting because the bi-Weibull shows a positive value while the tri-Weibull shows a negative value indicating they are skewed in opposite directions. However, the values are both close so the skewness isn't too far off despite the opposite signs. The PDF's are

shown in Figure 4.9 and do not indicate any significant difference in skewness as the close skewness values suggest.

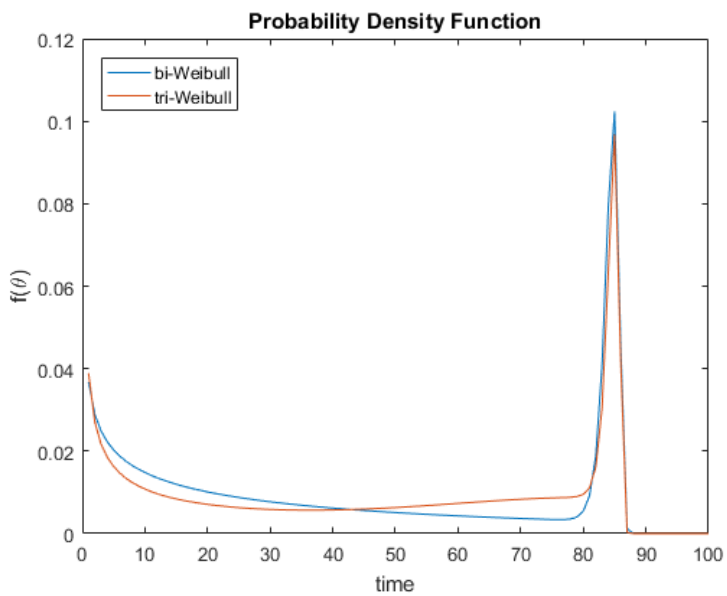

Figure 4.9: bi-Weibull & tri-Weibull PDF

The equations were both derived using the same methods and can be obtained from Eq. 2.28 for the general poly-Weibull. Comparing them to one another may render bias results. These results will need to be compared to other modified Weibull methods to better determine if the statistical properties are reasonable.

4.2 Computational Testing

The property values obtained for the bi-Weibull and tri-Weibull using the Taylor-series expansion equation derived will need to be examined further by comparing them to property values obtained for the Aarset data set for the EMWE (Eq. 2.22) & NMW (Eq. 2.18) as well as well as the bi-Weibull and tri-Weibull (Eq. 2.28) via numerical integration.

Table 4.4: Performance Measures for the Aarset Data Set

Model	**Parameters**	**Log-Lik**	**K-S**	**p-value**	**AIC**
bi-Weibull	4	−206.09	0.100	0.925	420.20
tri-Weibull	6	−202.51	0.063	0.998	417.01
NMW	5	−212.90	0.088	0.803	435.80
EMWE	4	−213.86	0.101	0.646	435.72

Table 4.4 displays a comparison of each models goodness of fit measures that were determined in [27]. This indicates that the null hypothesis of the two sample Kolmogorov-Smirnov Test (K-S) test cannot be rejected for any of the four models at a significance level below 0.8. However, the data also shows that the tri-Weibull and bi-Weibull fit the data better than either the NMW or the EMWE as both have larger likelihoods as well as smaller K-S statistics and Akaike Information Criterion (AIC) values. An interesting observation is that the tri-Weibull has the lowest AIC value despite having the most parameters. The model with the lowest AIC value is said to be the best fit but AIC is known to penalize models with higher parameters to prevent over-fitting. Despite the penalty obtained from the parameters, the tri-Weibull was still shown to be a better fit for the Aarset [26] data set.

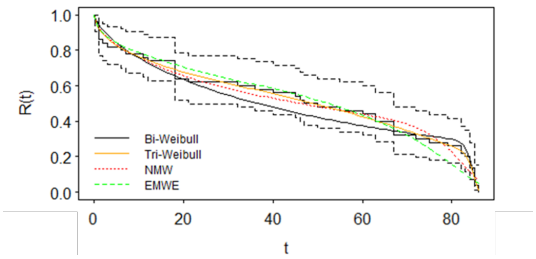

(a) Reliability function - Kaplan-Meier estimate

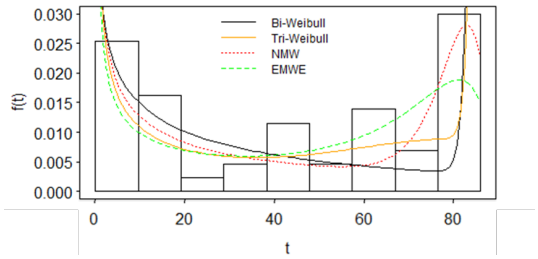

(b) PDF against Histogram

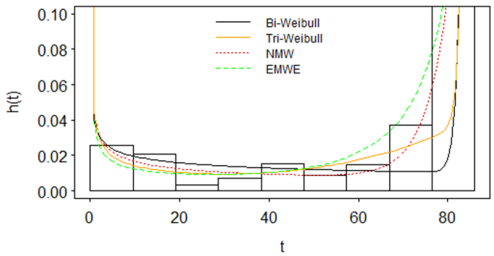

(c) Hazard Functions & Empirical Hazard Histogram

Figure 4.10: Comparing model fit for the Aarset data

Figure 4.10a shows the reliability function of each model plotted against the Kaplan-Meier estimate of the data. The NMW and EMWE are observed to fit the middle portion of the data better than the bi-Weibull. However, the lower and upper tails of the data show a better fit for both the bi-Weibull and tri-Weibull where the majority of observations are concentrated. The tri-Weibull is shown to be the best fit across the range of the observations. Figure 4.10b & 4.10c show the PDF plotted against a histogram of the data & the hazard functions plotted against the empirical hazard plot, respectively. In these two plots, it is evident that the the poly-Weibull models indicate that the probability of failure after the final observation is near zero, which is to be expected for a system with a true bathtubshaped hazard function, while the NMW and EMWE do not reflect this.

Table 4.5: MLE's for the Aarset Data Set

Model	**MLE of the Parameters**						
	α_1	α_2	α_3	β_1	β_2	β_3	λ
bi-Weibull	84.907	61.663		82.334	0.702		
tri-Weibull	85.091	92.299	122.478	98.152	4.215	0.524	
NMW	0.071	7.015×10^{-8}		0.016	0.595		0.197
EMWE	49.050	7.18×10^{-5}		3.148	0.145		

The MLE's for the Aarset Data Set are shown in Table 4.5 were determined in [27]. These values will be used with each respective equation to to determine their first four raw moments. The raw moments will then be used to determine the mean, variance, standard deviation, skewness, and kurtosis to be compared.

Table 4.6: Modified Weibull Raw Moment Values

	Numerical Integration				**Taylor-Series Approximation**	
Raw Moment	EMWE	NMW	bi-Weibull	tri-Weibull	bi-Weibull	tri-Weibull
$E[T]$	46.06922	45.15665	42.89954	45.79697	42.8995	45.9151
	(< 0.00061)	(< 0.00018)	(< 0.00075)	(< 0.0023)		
$E\left[T^2\right]$	3060.489	3123.966	2922.313	3144.316	2922.313	3160.356
	(< 0.0092)	(< 0.013)	(< 0.061)	(< 0.022)		
$E\left[T^3\right]$	221256.3	236630.4	223063.9	235784.7	223063.9	237477.3
	(< 0.89)	(< 1.1)	(< 5)	(< 1.9)		
$E\left[T^4\right]$	16656166	18570582	17777704	18370227	17777708	18533155
	(< 95)	(< 90)	(< 425)	(< 171)		

The values obtained using Eq. 3.5 are close to those calculated using numerical integration as shown in Table 4.6. Each raw moment for the bi-Weibull is almost an exact match between the two methods. The tri-Weibull shows an increasing difference between the numerically integrated value and the value from 3.5. The error associated with the bi-Weibull numerically integrated value is significantly high compared to the other methods.

Table 4.7: Modified Weibull Properties

		Numerical Integration			**Taylor-Series Approximation**	
Property	EMWE	NMW	bi-Weibull	tri-Weibull	bi-Weibull	tri-Weibull
μ	46.06922	45.15665	42.89954	45.79697	42.89953	45.91508
σ	30.62868	32.93695	32.89289	32.35666	32.89289	32.43704
$Var[T]$	938.116	1084.843	1081.942	1046.954	1081.943	1052.162
$Sk[T]$	−0.2148933	−0.06753683	0.1367966	−0.1213264	0.1367971	−0.1245532
$\kappa[T]$	1.526415	1.338853	1.373903	1.413325	1.373899	1.4095353

The statistical properties shown in Table 4.7 for each of the methods appear to all be very close. Each method renders similar values for the mean with the EMWE being the largest and bi-Weibull being the smallest (for both numerically integrated and using Eq. 3.5). The variance for each were close which lead to standard deviation values that are almost all the same to the nearest whole number; the only one with a dissimilar whole number is also the smallest (EMWE).

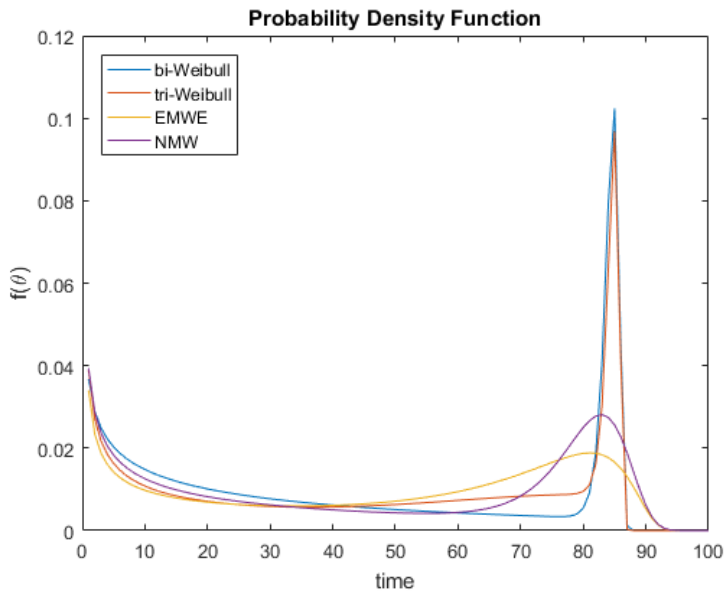

Figure 4.11: bi-Weibull, tri-Weibull, EMWE, & NMW PDF

It was observed in the last section that the skewness for the bi-Weibull and tri-Weibull are skewed in different directions; the bi-Weibull remains the only value with a positive skew for both the numerically integrated solution and the values obtained from Eq. 3.5. All of the values are close which suggests that the skewness is not too great (Figure 4.11) and each model is relatively symmetric, with NMW being the most symmetric and EMWE being skewed the most. The kurtosis for each method are very similar and indicates that each is platykurtic.

V. Conclusion & Future Work

5.1 Conclusion

The warfighting domain is changing and defense systems will continue to grow in complexity, which suggests that the number of embedded potential failure modes will also increase. In an effort to maintain its standing as the dominant military leader and protect the nations interests, the United States will need to ensure that all defense systems are reliable and fully functional to complete the mission, despite the increasing complexity and challenges that lie ahead.

Although a closed-form solution to the poly-Weibull moments was not possible using the methods shown in section 2.4, the Taylor-Series approximation produces logical values that can be used to estimate time for repairs, replacements, and scheduled maintenance. The derived equation can be tested against more data-sets to solidify the claim of validity. Eq. 3.5 is flexible with higher orders of poly-Weibull than the bi-Weibull and tri-Weibull should someone want to go higher than a tri-Weibull. The mathematical methods applied to obtain Eq. 3.5 are outlined such that they can easily understood so other may use them in deriving an estimated equation for the moments for any future developments.

It was determined in [27] that the poly-Weibull was a better fit for the Aarset data set that both the NMW and EMWE based on the values shown in Table 4.4. Since the statistical properties in Table 4.7 show little variation between them and the poly-Weibull has been shown to be a better fit to the data, it suffices to say that the properties obtained from Eq. 3.5 are acceptable.

5.2 Future Work

Many of the methods in this paper were tested against the Aarset data set **(author?)** [26]. This data set has a known bathtub-shaped hazard function that has been utilized in

many research papers when comparing modified Weibull distributions. Further research into more data sets with known bathtub-shaped hazard functions would provide a stronger argument for any of the modified-Weibull methods mentioned.

As stated in the introduction, these failures compete with each other. Some failures never occur in test because of other dominant failure modes. The method of moments will lead to an estimation of the population mean whereas testing results in a sample mean. Because of this, a mean can only be somewhat informative. For testing, a median may be a more useful statistic to obtain. Determining a median for the poly-Weibull would not be an easy tasks but would be value-added.

The end product of this research and the research by J.K Freels in [27] is to develop an package in R™ that will compare goodness-of-fit and determine the statistical properties.

Appendix A: Math Tools & Extra Derivations

A.1 Math Tools Applied

$$\text{Expected Value Equation: } E\left[t^k\right] = \int_0^\infty t^k f(t)dt \tag{A.1}$$

$$\text{First Law of Exponents: } e^{\sum a_i} = \prod e^{a_i} \tag{A.2}$$

$$\text{Gamma Function: } \Gamma(k) = \int_0^\infty t^{-k} \exp[-t]\, dt \tag{A.3}$$

$$\text{UV Substitution: } uv - \int vdu \tag{A.4}$$

$$\begin{aligned}\text{Termwise Integration: } \int \sum \alpha_i t dt &= \int (\alpha_1 + \alpha_2 + ... + \alpha_n)dt \\ &= \int \alpha_1 t dt + \int \alpha_2 t dt + ... \int \alpha_n t dt \\ &= \sum \int \alpha_i t dt\end{aligned} \tag{A.5}$$

A.2 Two-Parameter Weibull Moment Derivation

For a standard Weibull, the CDF is given by:

$$F(t|\alpha,\beta) = 1 - \exp\left[-\left(\frac{t}{\beta}\right)^\alpha\right]$$

The PDF is the derivative of the CDF:

$$\frac{d}{dt}F(t|\alpha,\beta) = \alpha\left(\frac{t}{\beta}\right)^{\alpha-1}\frac{1}{\beta}\exp\left[-\left(\frac{t}{\beta}\right)^\alpha\right] = \frac{\alpha}{\beta^\alpha}t^{\alpha-1}\exp\left[-\left(\frac{t}{\beta}\right)^\alpha\right] = f(t|\alpha,\beta)$$

Using $E\left(t^k\right) = \int_0^\infty t^k f(t)\, dt$

$$E\left(t^k\right) = \int_0^\infty t^k f(t)\, dt = \int_0^\infty t^k \frac{\alpha}{\beta^\alpha}t^{\alpha-1}\exp\left[-\left(\frac{t}{\beta}\right)^\alpha\right]dt$$

Let $u = \left(\frac{t}{\beta}\right)^\alpha$

$$u = \left(\frac{t}{\beta}\right)^{\alpha} \qquad\qquad du = \frac{\alpha}{\beta^{\alpha}} t^{\alpha-1} dt$$

Now, we multiply t^k by 1 where $\frac{\beta^k}{\beta^k} = 1$

$$t^k \left(\frac{\beta^k}{\beta^k}\right) = \beta^k \frac{t^k}{\beta^k} = \beta^k \left(\frac{t}{\beta}\right)^k$$

Next, we raise this to a power of 1, where $\frac{\alpha}{\alpha} = 1$

$$\beta^k \left(\frac{t}{\beta}\right)^k = \beta^k \left(\left(\frac{t}{\beta}\right)^k\right)^{\alpha/\alpha} = \beta^k \left(\left(\frac{t}{\beta}\right)^{\alpha}\right)^{k/\alpha}$$

Since we let $u = \left(\frac{t}{\beta}\right)^{\alpha}$, we solve this for t

$$t^k = \beta^k u^{k/\alpha}$$

Next, we return to the integral:

$$\int_0^{\infty} t^k \frac{\alpha}{\beta^{\alpha}} t^{\alpha-1} \exp\left[-\left(\frac{t}{\beta}\right)^{\alpha}\right] dt = \int_0^{\infty} \left(t^k\right)\left(\frac{\alpha}{\beta^{\alpha}} t^{\alpha-1} dt\right)\left(\exp\left[-\left(\frac{t}{\beta}\right)^{\alpha}\right]\right)$$

$$[= \int_0^{\infty} \left(\beta^k u^{\frac{k}{\alpha}}\right)(du)\left(\exp\left[-u\right]\right) = \int_0^{\infty} \beta^k u^{\frac{k}{\alpha}} \exp\left[-u\right] du]$$

Then, add 0 to the exponent of u, where $0 = 1 - 1$

$$\int_0^{\infty} \beta^k u^{\frac{k}{\alpha}+1-1} \exp\left[-u\right] du = \int_0^{\infty} \beta^k u^{\left(\frac{k}{\alpha}+1\right)-1} \exp\left[-u\right] du = \beta^k \int_0^{\infty} u^{\left(\frac{k}{\alpha}+1\right)-1} \exp\left[-u\right] du$$

This now resembles the integral for the Gamma Distribution:

$$\Gamma(\beta) = \int_{-\infty}^{\infty} t^{\beta-1} \exp\left[-t\right] dt$$

$$\beta^k \int_0^{\infty} u^{\left(\frac{k}{\alpha}+1\right)-1} \exp\left[-u\right] du = \beta^k \Gamma\left(\frac{k}{\alpha} + 1\right)$$

A.3 Obtaining Statistics from Raw Moments

A.3.1 Linearity of Expected Value.

If we have a probability space $(\Omega, \mathcal{F}, \mathcal{P})$, then the Expected Value of a random variable $T : \Omega \to \mathbb{R}$ is defined as:

$$E[T] = \int_{\Omega} T(\omega) dP(\omega)$$

Recall, that it is only well-defined if the integral converges absolutely, i.e.:

$$\int_{\Omega} |T(\omega)| dP(\omega) < \infty$$

If the Expected Values for T & X exists, then via the triangle inequality $E[T + X]$ exists. Since the integral is a Lebesgue integral, then for constants $a, b \in \mathbb{R}$ the linearity of the Lebesgue integral can be used to conclude:

$$E[aT + bX] = \int_{\Omega} aT + bX dP = \int_{\Omega} aT dP + \int_{\Omega} bX dP = a \int_{\Omega} T dP + b \int_{\Omega} X dP = aE[T] + bE[X] \quad \square$$

A.3.2 First Four Raw Moment & Mean.

First Raw Moment:	$E[t] = \mu$ (Mean)
Second Raw Moment:	$E\left[t^2\right]$
Third Raw Moment:	$E\left[t^3\right]$
Fourth Raw Moment:	$E\left[t^4\right]$

A.3.3 First Central Moment.

The expected value

$$E[t - \mu] = E[t] - E[\mu] = E[t] - \mu$$

A.3.4 Second Central Moment & Variance.

$$E\left[(t - \mu)^2\right] = E\left[t^2 - 2t\mu + \mu^2\right]$$

$$
\begin{aligned}
&= E\left[t^2\right] - E\left[2t\mu\right] + E\left[\mu^2\right] \\
&= E\left[t^2\right] - 2\mu E\left[t\right] + \mu^2 \\
&= E\left[t^2\right] - 2\mu\mu + \mu^2 \\
&= E\left[t^2\right] - 2\mu^2 + \mu^2 \\
&= E\left[t^2\right] - \mu^2
\end{aligned}
$$

The second central moment gives the variance.

$$Var[t] = E\left[t^2\right] - \mu^2 = \sigma^2$$

The standard deviation can be determined from the variance.

$$\sigma = \sqrt{Var[t]} = \sqrt{E\left[t^2\right] - \mu^2}$$

A.3.5 Third Central Moment & Skewness.

$$
\begin{aligned}
E\left[(t-\mu)^3\right] &= E\left[(t-\mu)^2(t-\mu)\right] \\
&= E\left[\left(t^2 - 2t\mu + \mu^2\right)(t-\mu)\right] \\
&= E\left[t^3 + t^2\mu - 2t^2\mu - 2t\mu^2 + t\mu^2 + \mu^3\right] \\
&= E\left[t^3 - t^2\mu - t\mu^2 + \mu^3\right] \\
&= E\left[t^3\right] - E\left[t^2\mu\right] - E\left[t\mu^2\right] + E\left[\mu^3\right] \\
&= E\left[t^3\right] - \mu E\left[t^2\right] - \mu^2 E\left[t\right] + \mu^3 \\
&= E\left[t^3\right] - \mu E\left[t^2\right] - \mu^2\mu + \mu^3 \\
&= E\left[t^3\right] - \mu E\left[t^2\right] + \mu^3 - \mu^2\mu \\
&= E\left[t^3\right] - \mu\left(E\left[t^2\right] - \mu^2\right) - \mu^3 \\
&= E\left[t^3\right] - \mu Var\left[t\right] - \mu^3
\end{aligned}
$$

The third central moment is used to determine skewness. The third central moment is normalized with respect to the standard deviation cubed.

$$Sk[t] = \frac{E\left[t^3\right] - \mu Var\left[t\right] - \mu^3}{\sigma^3}$$

A.3.6 Fourth Central Moment & Kurtosis.

$$\begin{aligned}
E\left[(t-\mu)^4\right] &= E\left[(t-\mu)^2(t-\mu)^2\right] \\
&= E\left[\left(t^2 - 2t\mu + \mu^2\right)\left(t^2 - 2t\mu + \mu^2\right)\right] \\
&= E\left[t^4 - 2t^3\mu + t^2\mu^2 - 2t^3\mu + 4t^2\mu^2 - 2t\mu^3 + t^2\mu^2 - 2t\mu^3 + \mu^4\right] \\
&= E\left[t^4 - 4t^3\mu + 6t^2\mu^2 - 4t\mu^3 + \mu^4\right] \\
&= E\left[t^4\right] - E\left[4t^3\mu\right] + E\left[6t^2\mu^2\right] - E\left[4t\mu^3\right] + E\left[\mu^4\right] \\
&= E\left[t^4\right] - 4\mu E\left[t^3\right] + 6\mu^2 E\left[t^2\right] - 4\mu^3 E\left[t\right] + \mu^4 \\
&= E\left[t^4\right] - 4\mu E\left[t^3\right] + 6\mu^2 E\left[t^2\right] - 4\mu^3\mu + \mu^4 \\
&= E\left[t^4\right] - 4\mu E\left[t^3\right] + 6\mu^2 E\left[t^2\right] - 4\mu^4 + \mu^4 \\
&= E\left[t^4\right] - 4\mu E\left[t^3\right] + 6\mu^2 E\left[t^2\right] - 3\mu^4
\end{aligned}$$

The fourth central moment is used to determine kurtosis. The fourth central moment is normalized with respect to the standard deviation to the fourth power.

$$\kappa[t] = \frac{E\left[t^4\right] - 4\mu E\left[t^3\right] + 6\mu^2 E\left[t^2\right] - 3\mu^4}{\sigma^4}$$

A.4 tri-Weibull Moment Derivation

We start with setting up the tri-Weibull distributions by setting $J = 3$:

$$f\left(t|\alpha_1, \alpha_2, \beta_1, \beta_2\right) = \exp\left[-\left(\frac{t}{\alpha_1}\right)^{\beta_1} - \left(\frac{t}{\alpha_2}\right)^{\beta_2} - \left(\frac{t}{\alpha_3}\right)^{\beta_3}\right]\left[\frac{\beta_1 t^{\beta_1 - 1}}{\alpha_1^{\beta_1}} + \frac{\beta_2 t^{\beta_2 - 1}}{\alpha_2^{\beta_2}} + \frac{\beta_3 t^{\beta_3 - 1}}{\alpha_3^{\beta_3}}\right]$$

Setting up the moment equation:

$$E\left(t^k\right) = \int_0^\infty t^k f\left(t|\alpha_1, \alpha_2, \beta_1, \beta_2\right) dt$$

Since we know the PDF is simply the derivative of the CDF (Eq. 1.4) and the CDF is contained in the PDF,

$$= \int_0^\infty t^k \exp\left[-\left(\frac{t}{\alpha_1}\right)^{\beta_1} - \left(\frac{t}{\alpha_2}\right)^{\beta_2} - \left(\frac{t}{\alpha_3}\right)^{\beta_3}\right]\left[\frac{\beta_1 t^{\beta_1-1}}{\alpha_1^{\beta_1}} + \frac{\beta_2 t^{\beta_2-1}}{\alpha_2^{\beta_2}} + \frac{\beta_3 t^{\beta_3-1}}{\alpha_3^{\beta_3}}\right] dt$$

we start by simplifying integral:

$$\exp\left[-\left(\frac{t}{\alpha_1}\right)^{\beta_1} - \left(\frac{t}{\alpha_2}\right)^{\beta_2} - \left(\frac{t}{\alpha_3}\right)^{\beta_3}\right]\left[\frac{\beta_1 t^{\beta_1-1}}{\alpha_1^{\beta_1}} + \frac{\beta_2 t^{\beta_2-1}}{\alpha_2^{\beta_2}} + \frac{\beta_3 t^{\beta_3-1}}{\alpha_3^{\beta_3}}\right]$$

$$= -\frac{d}{dt}\exp\left[-\left(\frac{t}{\alpha_1}\right)^{\beta_1} - \left(\frac{t}{\alpha_2}\right)^{\beta_2} - \left(\frac{t}{\alpha_3}\right)^{\beta_3}\right]$$

$$\rightarrow \int_0^\infty t^k\left(-\frac{d}{dt}\exp\left[-\left(\frac{t}{\alpha_1}\right)^{\beta_1} - \left(\frac{t}{\alpha_2}\right)^{\beta_2} - \left(\frac{t}{\alpha_3}\right)^{\beta_3}\right]\right) dt$$

Next, we assign terms to u and dv and take the derivative of u and anti-derivative of dv:

$$u = t^k \qquad dv = -\frac{d}{dt}\exp\left[-\left(\frac{t}{\alpha_1}\right)^{\beta_1} - \left(\frac{t}{\alpha_2}\right)^{\beta_2} - \left(\frac{t}{\alpha_3}\right)^{\beta_3}\right] dt$$

$$du = kt^{k-1}dt \qquad v = -\exp\left[-\left(\frac{t}{\alpha_1}\right)^{\beta_1} - \left(\frac{t}{\alpha_2}\right)^{\beta_2} - \left(\frac{t}{\alpha_3}\right)^{\beta_3}\right]$$

Now, we plug into $uv - \int vdu$

$$= \left\{-t^k \exp\left[-\left(\frac{t}{\alpha_1}\right)^{\beta_1} - \left(\frac{t}{\alpha_2}\right)^{\beta_2} - \left(\frac{t}{\alpha_3}\right)^{\beta_3}\right]\right\}_0^\infty + \int_0^\infty kt^{k-1}\exp\left[-\left(\frac{t}{\alpha_1}\right)^{\beta_1} - \left(\frac{t}{\alpha_2}\right)^{\beta_2} - \left(\frac{t}{\alpha_3}\right)^{\beta_3}\right] dt$$

Just as with the bi-Weibull, the left-hand-side of the equation goes to 0 when the limits are evaluated and we are left to solve only the right-hand-side.

$$= k\int_0^\infty t^{k-1}\exp\left[-\left(\frac{t}{\alpha_1}\right)^{\beta_1}-\left(\frac{t}{\alpha_2}\right)^{\beta_2}-\left(\frac{t}{\alpha_3}\right)^{\beta_3}\right]dt$$

We start with breaking up the exponents since: $e^{\sum a_i} = \prod e^{a_i}$

$$= k\int_0^\infty t^{k-1}\exp\left[-\left(\frac{t}{\alpha_1}\right)^{\beta_1}\right]\exp\left[-\left(\frac{t}{\alpha_2}\right)^{\beta_2}\right]\exp\left[-\left(\frac{t}{\alpha_3}\right)^{\beta_3}\right]dt$$

We only apply the Taylor-Series Expansion to the second and third exponential terms. We retain only the first exponential term to eventually build towards a gamma function the same way the bi-Weibull was done.

$$= k\int_0^\infty t^{k-1}\exp\left[-\left(\frac{t}{\alpha_1}\right)^{\beta_1}\right]\sum_{n_1=0}^{\infty}\frac{\left(-\left(\frac{t}{\alpha_2}\right)^{\beta_2}\right)^{n_1}}{n_1!}dt\sum_{n_2=0}^{\infty}\frac{\left(-\left(\frac{t}{\alpha_3}\right)^{\beta_3}\right)^{n_2}}{n_2!}dt$$

The next few steps involve algebraic manipulation to the equation to obtain a form that resembles the gamma function, $\Gamma(\beta) = \int_0^\infty t^{\beta-1}\exp[-t]\,dt$

$$= k\int_0^\infty t^{k-1}\exp\left[-\left(\frac{t}{\alpha_1}\right)^{\beta_1}\right]\sum_{n_1=0}^{\infty}\frac{\left(-\frac{t^{\beta_2}}{\alpha_2^{\beta_2}}\right)^{n_1}}{n_1!}\sum_{n_2=0}^{\infty}\frac{\left(-\frac{t^{\beta_3}}{\alpha_3^{\beta_3}}\right)^{n_2}}{n_2!}dt$$

The summation and terms not attached to the time variable t are pulled out of the integral followed by combining the t terms.

$$= k\sum_{n_1=0}^{\infty}\frac{1}{\left(-\alpha_2^{\beta_2}\right)^{n_1}n_1!}\sum_{n_2=0}^{\infty}\frac{1}{\left(-\alpha_3^{\beta_3}\right)^{n_2}n_2!}\int_0^\infty t^{k-1}\exp\left[-\left(\frac{t}{\alpha_1}\right)^{\beta_1}\right]t^{n_1\beta_2}t^{n_2\beta_3}dt$$

$$= k\sum_{n_1=0}^{\infty}\sum_{n_2=0}^{\infty}\frac{1}{\left(-\alpha_2^{\beta_2}\right)^{n_1}n_1!}\frac{1}{\left(-\alpha_3^{\beta_3}\right)^{n_2}n_2!}\int_0^\infty t^{k+n_1\beta_2+n_2\beta_3-1}\exp\left[-\left(\frac{t}{\alpha_1}\right)^{\beta_1}\right]dt$$

Next, we let $u = \left(\frac{t}{\alpha_1}\right)^{\beta_1}$, (term inside of the exponent) and take the derivative to obtain du

$$u = \left(\frac{t}{\alpha_1}\right)^{\beta_1}$$

$$du = \frac{\beta_1 t^{\beta_1 - 1}}{\alpha_1^{\beta_1}} dt = \frac{\beta_1 t^{\beta_1}}{\alpha_1^{\beta_1} t} dt$$

This term is solved for dt and plugged into the integral along with u. The t^{-1} cancels with the t in $t^{k+n\beta_2-1}$.

$$\rightarrow dt = \frac{\alpha_1^{\beta_1} t}{\beta_1 t^{\beta_1}} du = \frac{t}{\beta_1}\left(\frac{\alpha_1^{\beta_1}}{t^{\beta_1}}\right) du = \frac{t}{\beta_1}\left(\frac{\alpha_1}{t}\right)^{\beta_1} du = \frac{t}{u\beta_1} du$$

$$= k \sum_{n_1=0}^{\infty} \sum_{n_2=0}^{\infty} \frac{1}{\left(-\alpha_2^{\beta_2}\right)^{n_1} \left(-\alpha_3^{\beta_3}\right)^{n_2} n_1! n_2!} \int_0^{\infty} t^{k+n_1\beta_2+n_2\beta_3-1} \exp\left[-u\right] \left(\frac{t}{u\beta_1} du\right)$$

$$= \frac{k}{\beta_1} \sum_{n_1=0}^{\infty} \sum_{n_2=0}^{\infty} \frac{1}{\left(-\alpha_2^{\beta_2}\right)^{n_1} \left(-\alpha_3^{\beta_3}\right)^{n_2} n_1! n_2!} \int_0^{\infty} t^{k+n_1\beta_2+n_2\beta_3} \exp\left[-u\right] u^{-1} du$$

Rearranging $u = \left(\frac{t}{\alpha_1}\right)^{\beta_1}$, we get

$$\rightarrow \alpha_1 u^{1/\beta_1} = t$$

which we plug into the integral for t. The α_1 term is pulled out of the integral and u^{-1} is combined with $u^{(k+n\beta_2)/\beta_1}$.

$$= \frac{k}{\beta_1} \sum_{n_1=0}^{\infty} \sum_{n_2=0}^{\infty} \frac{1}{\left(-\alpha_2^{\beta_2}\right)^{n_1} \left(-\alpha_3^{\beta_3}\right)^{n_2} n_1! n_2!} \int_0^{\infty} \left(\alpha_1 u^{1/\beta_1}\right)^{k+n_1\beta_2+n_2\beta_3} \exp\left[-u\right] u^{-1} du$$

$$= \frac{k}{\beta_1} \sum_{n_1=0}^{\infty} \sum_{n_2=0}^{\infty} \frac{\alpha_1^{k+n_1\beta_2+n_2\beta_3}}{\left(-\alpha_2^{\beta_2}\right)^{n_1} \left(-\alpha_3^{\beta_3}\right)^{n_2} n_1! n_2!} \int_0^{\infty} u^{(k+n_1\beta_2+n_2\beta_3)/\beta_1} \exp\left[-u\right] u^{-1} du$$

$$= \frac{k}{\beta_1} \sum_{n_1=0}^{\infty} \sum_{n_2=0}^{\infty} \frac{\alpha_1^{k+n_1\beta_2+n_2\beta_3}}{\left(-\alpha_2^{\beta_2}\right)^{n_1} \left(-\alpha_3^{\beta_3}\right)^{n_2} n_1! n_2!} \int_0^{\infty} u^{\frac{k+n_1\beta_2+n_2\beta_3}{\beta_1}-1} \exp\left[-u\right] du$$

Now, the integral is in the form of a gamma function.

$$= \frac{k}{\beta_1} \sum_{n_1=0}^{\infty} \sum_{n_2=0}^{\infty} \frac{\alpha_1^{k+n_1\beta_2+n_2\beta_3}}{\left(-\alpha_2^{\beta_2}\right)^{n_1} \left(-\alpha_3^{\beta_3}\right)^{n_2} n_1! n_2!} \Gamma\left(\frac{k + n_1\beta_2 + n_2\beta_3}{\beta_1}\right)$$

Appendix B: Code

B.1 Mean, Variance, Skewness, & Kurtosis Code

B.1.1 bi-Weibull Taylor Series Approximation Code.

```
clc; clear all; close all;
% Values
a1 = 84.907;  a2 = 61.663;  b1 = 82.334;  b2 = 0.702;
```

B.1.1.1 Mean.

```
n = 0; nn = []; delall = 1; tol = 1e-4; % setting initial count,
% creating vector, tolerance, & creating delta value
% to reset to after each loop

calc = ((a1^(n*b2))/(((-a2^b2)^n)*factorial(n)))*gamma((1+n*b2)/b1);
% initial calculation for n=0
del = delall;

sumvec1 = [];
sum1 = calc; % creating initial sum value

while abs(del) > tol

    sumvec1(n+1) = sum1; % adding each calculation to vector
    nn(n+1) = n+1; % next value for n vector within loop
    n = n+1; % next value for n within loop

    calc2 = ((a1^(n*b2))/(((-a2^b2)^n)*factorial(n)))*gamma((1+n*b2)/b1);
```

```
    sum1 = sum1 + calc2; % adding to sum

    del = calc2 - calc; % determing difference for tolerance

    calc = calc2; % changing calculated value for next delta determination

end

Et        = (a1/b1)*sumvec1(end); % first raw moment
bwmean    = Et; % mean for bi-Weibull
Etvec     = (a1/b1)*sumvec1; % first raw moment vector
bwmeanvec = Etvec; % mean vector to see covergence
```

B.1.1.2 Variance.

```
m  = 0; mm = []; % setting sum value and vector

calc3 = ((a1^(m*b2))/(((-a2^b2)^m)*factorial(m)))*gamma((2+m*b2)/b1);
% initial calculation for m=0
del2 = delall;

sumvec2 = [];
sum2 = calc3; % initial value for sum

while abs(del2) > tol

    sumvec2(m+1) = sum2; % adding each calculation to vector
```

```
    mm(m+1) = m+1; % adding next term for vector
    m = m+1; % adding next vector

    calc4 = ((a1^(m*b2))/(((-a2^b2)^m)*factorial(m)))*gamma((2+m*b2)/b1);
    % calculation within loop

    sum2 = sum2 + calc4; % adding new calculation to sum

    del2 = calc4 - calc3; % taking difference between subsequence churns
    % for tolerance

    calc3 = calc4; % resetting prior calculated term for tolerance determination

end

Et2          = ((2*(a1^2))/b1)*sumvec2(end); % second raw moment
Et2vec       = ((2*(a1^2))/b1)*sumvec2; % 2nd raw moment vector
biweibvar    = Et2 - Et^2; % variance calculation
biweibvarvec = Et2vec - bwmeanvec.^2; % variance vector to determine convergence

bwsd    = sqrt(biweibvar); % standard deviation calculation
bwsdvec = sqrt(biweibvarvec); % standard deviation vector for convergence
```

B.1.1.3 Skewness.

```
l = 0; ll = []; % setting sum value and vector

calc5 = ((a1^(l*b2))/(((-a2^b2)^l)*factorial(l)))*gamma((3+l*b2)/b1);
```

```
% initial calculation for l=0
del3 = delall; % setting del for new calculations

sumvec3 = []; % creating sum vector
sum3 = calc5; % setting initial sum value

while abs(del3) > tol

    sumvec3(l+1) = sum3; % placing calculation into vector
    ll(l+1) = l+1; % adding next term in vector
    l = l+1; % adding next term for sum

    calc6 = ((a1^(l*b2))/(((-a2^b2)^l)*factorial(l)))*gamma((3+l*b2)/b1);
    % calculation for each value of l

    sum3 = sum3 + calc6; % adding to sum

    del3 = calc6 - calc5;
    % taking difference of subsequent calculations to check tolerace

    calc5 = calc6; % resetting calculation value for next churn

end

Et3           = ((3*(a1^3))/b1)*sumvec3(end); % 3rd raw moment
Et3vec        = ((3*(a1^3))/b1)*sumvec3; % 3rd raw moment vector
```

```
biweibskew    = (Et3-3*Et*biweibvar-Et^3)/bwsd^3; % Skewness
biweibskewvec = (Et3vec-3*Etvec.*biweibvarvec-Et.^3)./bwsdvec.^3;
% skewness vector for convergence
```

B.1.1.4 Kurtosis.

```
k = 0; kk = []; % setting initial value and vector

calc7 = ((a1^(k*b2))/(((-a2^b2)^k)*factorial(k)))*gamma((4+k*b2)/b1);
% initial calculation
del4 = delall;

sumvec4 = []; % creating vector
sum4 = calc7; % setting first term for sum

while abs(del4) > tol

    sumvec4(k+1) = sum4;
    % placing calculated value into sum vector
    kk(k+1) = k+1; % next value for sum vector

    k = k+1; % next value for sum

    calc8 = ((a1^(k*b2))/(((-a2^b2)^k)*factorial(k)))*gamma((4+k*b2)/b1);
    % inner loop calculation

    sum4 = sum4 + calc8; % adding new calc to sum
```

```
    del4 = calc8 - calc7;
    % difference of subsequent calculation for tolerance

    calc7 = calc8; % resetting calculated value for next churn

end

Et4       = ((4*(a1^4))/b1)*sumvec4(end); % 4th raw moment
Et4vec    = ((4*(a1^4))/b1)*sumvec4; % 4th raw moment vector
bwkurt    = (Et4-4*Et*Et3+6*(Et^2)*Et2-3*Et^4)/bwsd^4; % kurtosis
bwkurtvec = (Et4vec-4*Etvec.*Et3vec+6*(Etvec.^2).*Et2vec-3*Etvec.^4)./bwsdvec.^4;
% kurtsosis vector for convergence
```

B.1.1.5 Plots.

```
figure
plot(nn,bwmeanvec,mm,bwsdvec);
xlabel('Iterations')
ylabel('\mu , \sigma')
title('bi-Weibull Mean & Standard Deviation Convergence')
legend('Mean','Standard Deviation')
axis([1 length(nn) 0 100])

figure
plot(nn,bwmeanvec,mm,bwsdvec);
xlabel('Iterations')
ylabel('\mu , \sigma')
title('bi-Weibull Mean & Standard Deviation Convergence')
```

```
legend('Mean','Standard Deviation')
axis([1 length(nn) 32 43])

figure
plot(mm,biweibvarvec);
xlabel('Iterations')
ylabel('Var(t)')
title('bi-Weibull Variance Convergence')
axis([1 length(mm) 0 1400])

figure
plot(mm,biweibvarvec);
xlabel('Iterations')
ylabel('Var(t)')
title('bi-Weibull Variance Convergence')
axis([1 length(mm) 1080 1082])

figure
plot(ll,biweibskewvec);
xlabel('Iterations')
ylabel('sk(t)')
title('bi-Weibull Skewness Convergence')

figure
plot(ll,biweibskewvec);
xlabel('Iterations')
```

```
ylabel('sk(t)')
title('bi-Weibull Skewness Convergence')
axis([1 length(ll) -0.5e5 2.5e5])

figure
plot(ll,biweibskewvec);
xlabel('Iterations')
ylabel('sk(t)')
title('bi-Weibull Skewness Convergence')
axis([1 length(ll) -.2 .2])

figure
plot(ll,biweibskewvec);
xlabel('Iterations')
ylabel('sk(t)')
title('bi-Weibull Skewness Convergence')
axis([1 length(ll) .1 .15])

figure
plot(kk,bwkurtvec);
xlabel('Iterations')
ylabel('\kappa')
title('bi-Weibull Kurtosis Convergence')

figure
plot(kk,bwkurtvec);
```

```
xlabel('Iterations')
ylabel('\kappa')
title('bi-Weibull Kurtosis Convergence')
axis([1 length(kk) -1000 100])

figure
plot(kk,bwkurtvec);
xlabel('Iterations')
ylabel('\kappa')
title('bi-Weibull Kurtosis Convergence')
axis([1 length(kk) 0 2])

figure
plot(kk,bwkurtvec);
xlabel('Iterations')
ylabel('\kappa')
title('bi-Weibull Kurtosis Convergence')
axis([1 length(kk) 1.3 1.4])
```

B.1.2 tri-Weibull Taylor Series Approximation Code.

```
clc; clear all; close all;
% MLE Parameter Values
a1 = 85.091;  a2 = 122.478;  a3 = 92.999;
b1 = 98.152;  b2 = 0.524;    b3 = 4.215;
% Initial delta and tolerance
tol = 1e-4; delall = 1;
```

B.1.2.1 Mean.

```
n1  = 0; nn1 = []; % creating initial values and
n2  = 0; nn2 = []; % vectors for inner and outer sum

calcm1 = ((a1^(n1*b2+n2*b3))/(((-a2^b2)^n1)*((-a3^b3)^n2)*factorial(n1)
       *factorial(n2)))*gamma((1+n1*b2+n2*b3)/b1);
       % initial calculation for n1=0 n2=0
delm1 = delall;

outsumet1 = []; % creating initial vectors
insumet1 = [];
sumet1 = calcm1; % setting first value for sum

while abs(delm1) > tol % outer sum
    nn1(n1+1) = n1+1; % next value for outer sum vector
    delm2 = delall; % reset delta after loop

    while abs(delm2) > tol % inner sum
        insumet1(n2+1,n1+1) = sumet1; % inner sum vector
        nn2(n2+1,n1+1) = n2+1; % next value for inner sum
        n2 = n2+1; % next value for inner sum


        calcm2 = ((a1^(n1*b2+n2*b3))/(((-a2^b2)^n1)*((-a3^b3)^n2)*factorial(n1)
               *factorial(n2)))*gamma((1+n1*b2+n2*b3)/b1);
        % inner sum calculation
```

```
        sumet1 = sumet1 + calcm2; % adding to inner sum
        delm2 = calcm2 - calcm1; % inner sum delta
        calcm1 = calcm2; % setting to last calculation

    end

    n2 =0; % resetting inner sum to 0
    outsumet1(n1+1) = sumet1; % outer sum vector
    n1 = n1+1; % outer sum value change

    calcm3 = ((a1^(n1*b2+n2*b3))/(((-a2^b2)^n1)*((-a3^b3)^n2)*factorial(n1)
           *factorial(n2)))*gamma((1+n1*b2+n2*b3)/b1);
    % outer sum calculation
    delm1 = calcm3 - calcm1; % check tolerance of outer sum
    sumet1 =  sumet1 + calcm3; % adding to total sum
    calcm1 =  calcm3; % set to last overall sum value

end


Et        = (a1/b1)*outsumet1(find(outsumet1,1,'last'));
% 1st raw moment
twmean    = Et; % mean

Etvec     = (a1/b1)*outsumet1; % 1st raw moment vector
Etvec     = Etvec(Etvec>0);
```

```
twmeanvec = Etvec; % mean vector
twmeanvec = twmeanvec(twmeanvec>0);
```

B.1.2.2 Variance.

```
m1  = 0; mm1 = []; % initial values and vectors
m2  = 0; mm2 = []; % for inner and outer sum

calcv1 = ((a1^(m1*b2+m2*b3))/(((-a2^b2)^m1)*((-a3^b3)^m2)*factorial(m1)
       *factorial(m2)))*gamma((2+m1*b2+m2*b3)/b1);
       % initial calculation for m1=0, m2=0
delv1 = delall;

outsumet2 = []; % outer sum vector
insumet2 = []; % inner sum vector
sumet2 = calcv1; % keeping initial calc for sum

while abs(delv1) > tol
    mm1(m1+1) = m1+1; % next number for outer sum vector
    delv2 = delall; % resetting delta for inner sum

    while abs(delv2) > tol
        insumet2(m2+1,m1+1) = sumet2;
        % saving calculation for inner sum vector
        mm2(m2+1,m1+1) = m2+1; % next inner sum vector
        m2 = m2+1; % setting next number for calc
```

```
        calcv2 = ((a1^(m1*b2+m2*b3))/(((-a2^b2)^m1)*((-a3^b3)^m2)*factorial(m1)
               *factorial(m2)))*gamma((2+m1*b2+m2*b3)/b1);
        % inner sum calculation
        sumet2 = sumet2 + calcv2; % adding to inner sum
        delv2 = calcv2 - calcv1;
        % delta for inner sum to check tolerance
        calcv1= calcv2; % setting to last calculated value

    end

    m2 =0; % resetting inner sum value
    outsumet2(m1+1) = sumet2;
    % saving value for outer sum vector
    m1 = m1+1; % next value for outer sum

    calcv3 = ((a1^(m1*b2+m2*b3))/(((-a2^b2)^m1)*((-a3^b3)^m2)*factorial(m1)
           *factorial(m2)))*gamma((2+m1*b2+m2*b3)/b1);
    % outer sum calculation with next value
    sumet2 = sumet2 + calcv3; % adding to total sum
    delv1  = calcv3 - calcv1;
    % overall delta to check tolerance
    calcv1 = calcv3; % setting to last calculated value

end

Et2    = ((2*(a1^2))/b1)*outsumet2(find(outsumet2,1,'last'));
```

```
twvar = Et2 - Et^2;
outsumet22 = outsumet2(outsumet2>0);
Et2vec = ((2*(a1^2))/b1)*outsumet22;
twvarvec = Et2vec - Etvec(1:length(Et2vec)).^2;

twsd = sqrt(twvar);
twsdvec = sqrt(twvarvec);

twvarvecin = ((2*(a1^2))/b1)*insumet2 - Et^2;
twvarvecin = twvarvecin.*(twvarvecin>0);
twsdvecin  = real(sqrt(twvarvecin));
```

B.1.2.3 Skewness.

```
l1  = 0; ll1 = []; % creating initial sum values and
l2  = 0; ll2 = []; % vector for inner and outer sum

calcs1 = ((a1^(l1*b2+l2*b3))/(((-a2^b2)^l1)*((-a3^b3)^l2)*factorial(l1)
       *factorial(l2)))*gamma((3+l1*b2+l2*b3)/b1);
       % initial calculation for l1=0 and l2=0
dels1 = delall;

outsumet3 = [];
insumet3 = [];
sumet3 = calcs1; % setting initial value in sum

while abs(dels1) > tol
    ll1(l1+1) = l1+1; % setting next vector value
```

```
dels2 = delall; % resetting inner sum delta

while abs(dels2) > tol
    insumet3(l2+1,l1+1) = sumet3;
    % saving inner sum vector
    ll2(l2+1,l1+1) = l2+1;
    % next value for inner sum vector
    l2 = l2+1; % next value for inner sum calculation



    calcs2 = ((a1^(l1*b2+l2*b3))/(((-a2^b2)^l1)*((-a3^b3)^l2)*factorial(l1)
           *factorial(l2)))*gamma((3+l1*b2+l2*b3)/b1);
    % inner sum calculation
    sumet3 = sumet3 + calcs2; % adding to inner sum
    dels2 = calcs2 - calcs1;
    % delta for inner sum tolerance check
    calcs1 = calcs2;
    % setting to new inner sum calculation

end

l2 =0; % resetting inner sum value
outsumet3(l1+1) = sumet3; % outer sum vector value change
l1 = l1+1; % updating outer sum value

calcs3 = ((a1^(l1*b2+l2*b3))/(((-a2^b2)^l1)*((-a3^b3)^l2)*factorial(l1)
```

```
            *factorial(l2)))*gamma((3+l1*b2+l2*b3)/b1);
         % outer sum calculation
    sumet3 = sumet3 + calcs3; % adding to overall sum
    dels1  = calcs3 - calcs1;
    % outer sum delta  for tolerance check
    calcs1 = calcs3; % updating for delta



end

Et3        = ((3*(a1^3))/b1)*outsumet3(find(outsumet3,1,'last'));
twsk       = (Et3-3*Et*twvar-Et^3)/twsd^3;
sumskvec3  = outsumet3(outsumet3>0);
Et3vec     = ((3*(a1^3))/b1)*sumskvec3;
twskvec    = (Et3vec-3*Etvec(1:length(Et3vec)).*twvarvec
           -Etvec(1:length(Et3vec)).^3)./twsdvec.^3;

Et3vecin  = ((3*(a1^3))/b1)*insumet3;
twskvecin = (Et3vecin-3*Et*twvar-Et^3)./twsdvecin.^3;
```

B.1.2.4 Kurtosis.

```
kk  = 0; kk1 = []; % initial values and vector for
k2  = 0; kk2 = []; % inner and outer sum

calck1 = ((a1^(kk*b2+k2*b3))/(((-a2^b2)^kk)*((-a3^b3)^k2)*factorial(kk)
       *factorial(k2)))*gamma((4+kk*b2+k2*b3)/b1);
       % initial calculation for k1=0 and k2=0
```

```
delk1 = delall; %calculate n1=0,n2=0

outsumet4 = []; % creating vector for outer sums
insumet4 = []; % creating vector for inner sums
sumet4 = calck1; % setting initial value in sum

while abs(delk1) > tol
    kk1(kk+1) = kk+1; % next value in outer sum vector
    delk2 = delall; % resetting delta for inner sum

    while abs(delk2) > tol
        insumet4(k2+1,kk+1) = sumet4;
        % saving inner sum value to vector
        kk2(k2+1,kk+1) = k2+1; %setting next vector value
        k2 = k2+1;
        % moving to next number in sum calculation



        calck2 = ((a1^(kk*b2+k2*b3))/(((-a2^b2)^kk)*((-a3^b3)^k2)*factorial(kk)
               *factorial(k2)))*gamma((4+kk*b2+k2*b3)/b1);
        % inner sum calculation
        sumet4 = sumet4 + calck2; % adding to inner sum
        delk2 = calck2 - calck1;
        % delta for inner some tolerance check
        calck1 = calck2;
        % setting to last calculation for next delta check
```

```
    end

    k2 =0; % resetting inner sum value
    outsumet4(kk+1) = sumet4;
    % setting outer sum value for vector
    kk = kk+1; % moving to next outer sum value

    calck3 = ((a1^(kk*b2+k2*b3))/(((-a2^b2)^kk)*((-a3^b3)^k2)*factorial(kk)
           *factorial(k2)))*gamma((4+kk*b2+k2*b3)/b1);
    % outer sum calculation
    sumet4 = sumet4 + calck3; % adding to total sum
    delk1  = calck3 - calck1;
    % delta taken for outer sum tolerance check
    calck1 = calck3;
    % setting to most recent calculation for next tolerance check

end

Et4          = ((4*(a1^4))/b1)*outsumet4(find(outsumet4,1,'last'));
twkurt       = (Et4-4*Et*Et3+6*(Et^2)*Et2-3*Et^4)/twsd^4;
sumkurtvec3  = outsumet4(outsumet4>0);
Et4vec       = ((4*(a1^4))/b1)*sumkurtvec3;
twkurtvec    = (Et4vec-4*Etvec(1:length(Et4vec)).*Et3vec
             +6*(Etvec(1:length(Et4vec)).^2).*Et2vec
             -3*Etvec(1:length(Et4vec)).^4)./twsdvec.^4;
```

```
Et4vec22     = ((4*(a1^4))/b1)*insumet4;
sumkurtvec22 = (Et4vec22-4*Et*Et3+6*(Et^2)*Et2-3*Et^4)/twsd^4;
```

B.1.2.5 Plots.

```
figure
plot(nn1(1:length(twmeanvec)),twmeanvec,mm1(1:length(twsdvec)),twsdvec);
xlabel('Iterations')
ylabel('\mu , \sigma')
title('tri-Weibull Mean & Standard Deviation Convergence')
legend('Mean','Standard Deviation')



figure
plot(mm1(1:length(twvarvec)),twvarvec);
xlabel('Iterations')
ylabel('Var(t)')
title('tri-Weibull Variance Convergence')
axis([1 length(twvarvec) 0 1200])

figure
plot(ll1(1:length(twskvec)),twskvec);
xlabel('Iterations')
ylabel('sk(t)')
title('tri-Weibull Skewness Convergence')

figure
```

```
plot(kk1(1:length(twkurtvec)),twkurtvec);
xlabel('Iterations')
ylabel('\kappa')
title('tri-Weibull Kurtosis Convergence')

N=nn2(:,1);
A=insumet1(:,1);A=A(A>0);B=insumet1(:,2);B=B(B>0);C=insumet1(:,3);C+C(C>0);
D=insumet1(:,4);D=D(D>0);E=insumet1(:,5);E=E(E>0);F=insumet1(:,6);F=F(F>0);
G=insumet1(:,7);G=G(G>0);H=insumet1(:,8);H=H(H>0);I=insumet1(:,9);I=I(I>0);
figure
plot(N(A>0),A,N(B>0),B,N(C>0),C,N(D>0),D,N(E>0),E,N(F>0),F,N(G>0),G,N(H>0),H,N(I>0)
xlabel('Iterations')
ylabel('\mu')
title('tri-Weibull Mean Convergence')
legend('n_1=0','n_1=1','n_1=2','n_1=3','n_1=4','n_1=5','n_1=6','n_1=7','n_1=8')
legend('location','northeast')

M=mm2(:,1);
A2=twvarvecin(:,1);A2=A2(A2>0);B2=twvarvecin(:,2);B2=B2(B2>0);
C2=twvarvecin(:,3);C2=C2(C2>0);D2=twvarvecin(:,4);D2=D2(D2>0);
E2=twvarvecin(:,5);E2=E2(E2>0);F2=twvarvecin(:,6);F2=F2(F2>0);
G2=twvarvecin(:,7);G2=G2(G2>0);H2=twvarvecin(:,8);H2=H2(H2>0);

figure
plot(M(A2>0),A2,M(B2>0),B2,M(C2>0),C2,M(D2>0),D2,M(E2>0),E2,M(F2>0),F2,M(G2>0),G2,M
xlabel('Iterations')
```

```
ylabel('Var(t)')
title('tri-Weibull Variance Convergence')
legend('n_1=0','n_1=1','n_1=2','n_1=3','n_1=4','n_1=5','n_1=6','n_1=7')
legend('location','northeast')


A3=twsdvecin(:,1);A3=A3(A3>0);B3=twsdvecin(:,2);B3=B3(B3>0);
C3=twsdvecin(:,3);C3=C3(C3>0);D3=twsdvecin(:,4);D3=D3(D3>0);
E3=twsdvecin(:,5);E3=E3(E3>0);F3=twsdvecin(:,6);F3=F3(F3>0);
G3=twsdvecin(:,7);G3=G3(G3>0);H3=twsdvecin(:,8);H3=H3(H3>0);

figure
plot(M(A3>0),A3,M(B3>0),B3,M(C3>0),C3,M(D3>0),D3,M(E3>0),E3,M(F3>0),F3,M(G3>0),G3,M
xlabel('Iterations')
ylabel('\sigma')
title('tri-Weibull Standard Deviation Convergence')
legend('n_1=0','n_1=1','n_1=2','n_1=3','n_1=4','n_1=5','n_1=6','n_1=7')
legend('location','northeast')



L=ll2(:,1);
A4=twskvecin(:,1);B4=twskvecin(:,2);C4=twskvecin(:,3);
D4=twskvecin(1:7,4);E4=twskvecin(1:6,5);F4=twskvecin(1:6,6);
G4=twskvecin(1:5,7);H4=twskvecin(1:3,8);
```

```
figure
plot(L,A4,L,B4,L,C4,L(1:7),D4,L(1:6),E4,L(1:6),F4,L(1:5),G4,L(1:3),H4);
xlabel('Iterations')
ylabel('sk(t)')
title('tri-Weibull Skewness Convergence')
legend('n_1=0','n_1=1','n_1=2','n_1=3','n_1=4','n_1=5','n_1=6','n_1=7')
legend('location','northeast')

figure
plot(L,A4,L,B4,L,C4,L(1:7),D4,L(1:6),E4,L(1:6),F4,L(1:5),G4,L(1:3),H4);
xlabel('Iterations')
ylabel('sk(t)')
title('tri-Weibull Skewness Convergence')
legend('n_1=0','n_1=1','n_1=2','n_1=3','n_1=4','n_1=5','n_1=6','n_1=7')
legend('location','northeast')
axis([1 length(L) -1 1.1])

K=kk2(:,1);
A5=sumkurtvec22(:,1);B5=sumkurtvec22(:,2);C5=sumkurtvec22(:,3);
D5=sumkurtvec22(1:7,4);E5=sumkurtvec22(1:6,5);F5=sumkurtvec22(1:6,6);
G5=sumkurtvec22(1:5,7);H5=sumkurtvec22(1:3,8);


figure
plot(K,A5,K,B5,K,C5,K(1:7),D5,K(1:6),E5,K(1:6),F5,K(1:5),G5,K(1:3),H5);
xlabel('Iterations')
```

```
ylabel('\kappa')
title('tri-Weibull Kurtosis Convergence')
legend('n_1=0','n_1=1','n_1=2','n_1=3','n_1=4','n_1=5','n_1=6','n_1=7')
legend('location','northeast')
```

B.1.3 bi-Weibull Numerical Integration Code.

```
bw_moment <- function(k = 1) {

  a1 = 84.907 ; b1 = 82.334
  a2 = 61.663 ; b2 = 0.702

  fun <- function(t) {

    term1 <- t ^ (k - 1)
    term2 <- exp(-(t / 84.907) ^ 82.334 - (t / 61.663) ^ 0.702)

    return(term1 * term2)

  }
  zout <- list()

  zout$int_full <- integrate(f = fun, lower = 0, upper = Inf)
  zout$int_value <- zout$int_full$value * k

  return(zout)

}
```

B.1.4 tri-Weibull Numerical Integration Code.

```
tw_moment <- function(k = 1) {

  a1 = 85.091 ;   b1 = 98.152
  a2 = 122.4787 ; b2 = 0.524
  a3 = 92.299 ;   b3 = 4.215

  fun <- function(t) {

    term1 <- t ^ (k - 1)
    term2 <- exp(-(t / a1) ^ b1 - (t / a2) ^ b2 - (t / a3) ^ b3)

    return(term1 * term2)

  }
  zout <- list()

  zout$int_full <- integrate(f = fun, lower = 0, upper = Inf)
  zout$int_value <- zout$int_full$value * k

  return(zout)

}
```

B.1.5 New Modified Weibull Numerical Integration Code.

```
nmw_moment <- function(k = 1) {
```

```
  a = 0.071 ;    l = 0.197
  B = 7.015e-8 ; Y = 0.016
  O = 0.595

  fun <- function(t) {

    term1 <- t ^ (k - 1)
    term2 <- exp(-a * t ^ O - B * t ^ Y * exp(l * t))

    return(term1 * term2)

  }
  zout <- list()

  zout$int_full <- integrate(f = fun, lower = 0, upper = Inf)
  zout$int_value <- zout$int_full$value * k

  return(zout)

}
```

B.1.6 Exponentiated Modified Weibull Extension Numerical Integration Code.

```
emwe_moment <- function(k = 1) {

  a = 49.050 ;   l = 7.18e-5
  B = 3.148 ; Y = 0.145
```

```
  fun <- function(t) {



    term1 <- t ^ (k+B-1)
    term2 <- exp((t / a) ^ B + l * a * (1 - exp((t / a) ^ B)))
    term3 <- (1 - exp(l * a * (1 - exp((t / a) ^ B)))) ^ (Y - 1)
    term4 <- (l*B*Y) / (a ^ (B-1))

    return(term1 * term2 * term3 * term4)

  }
  zout <- list()

  zout$int_full <- integrate(f = fun, lower = 0, upper = Inf)
  zout$int_value <- zout$int_full$value

  return(zout)

}
```

Appendix C: List of Acronyms

AAG	Advanced Arresting Gear
AIC	Akaike Information Criterion
BMW	Beta Modified Weibull
CFR	constant failure rate
CDF	Cumulative Distribution Function
DFR	decreasing failure rate
DoD	Department of Defense
EMWE	Exponentiated Modified Weibull Extension
EMALS	Electromagnetic-Powered Aircraft Launch System
FY	Fiscal Year
FMEA	Failure Modes Effects & Analysis
FMECA	Failure Mode, Effects, & Criticality Analysis
IFR	increasing failure rate
K-S	Kolmogorov-Smirnov Test
LFR	Linear Failure Rate
MDAPs	Major Defense Acquisition Programs
MLE	Maximum Likelihood Estimation
MTTF	Mean Time to Failure
MW	Modified Weibull
NMW	New Modified Weibull
PDF	Probability Density Function
RAM	Reliability, Availability, & Maintainability
RDT&E	Research, Development, Test, & Evaluation
RPA	Remotely Piloted Aircraft
S&T	Science & Technology
CVN 78	USS Gerald Ford
CVN 79	USS John F. Kennedy
CVN 80	USS Enterprise
WPP	Weibull Probability Paper

Bibliography

[1] C. Ebeling, *An Introduction to Reliability and Maintainability Engineering*. The McGraw-Hill Company, Inc., 1997.

[2] B. Blanchard and W. Fabrycky, *Systems Engineering and Analysis*. Pearson/Prentice Hall, 2011.

[3] W. Nelson, "Accelerated Testing: Statistical Models, Test Plans and Data Analyses," 1980.

[4] V. Pisacane, *The Space Environment and Its Effects on Space Systems*. American Institute of Aeronautics and Astronautics Education Series, 2016.

[5] J. Wertz, D. Everett, and J. Puschell, *Space Mission Engineering: The New SMAD*. Microcosm Press, 2015.

[6] W. Meeker and L. Escobar, *Statistical Methods for Reliability Data*. Wiley Interscience, 1998.

[7] D. A. Guide, "DoD Guide For Achieving Reliability, Availability, and Maintainability," *Acquisition, Technology, and Logistics*, 2005.

[8] G. Klutke, P. Kiessler, and M. Wortman, "A Critical Look at the Bathtub Curve," *IEEE Transactions on Reliability*, 2003.

[9] MIL-HDBK-338B, "Electronic Reliability Design Handbook," *Analysis Center*, 1992.

[10] MIL-HDBK-189A, "Reliability Growth Management," *Naval Publications and Forms Center*, 2011.

[11] "2018 Program Acquisition Costs by Weapon System," *United States FY Department of Defense Fiscal Year 2018 Budget Request*, 2018.

[12] M. Tafazoli, "A Study of On-Orbit Spacecraft Failures," *Acta Astronautica*, 2009.

[13] "2017 Program Acquisition Costs by Weapon System," *United States FY Department of Defense Fiscal Year 2017 Budget Request*, 2017.

[14] Z. Cohen, "Sneak Peek at US Navy's New $13B Aircraft Carrier," *CNN*.

[15] A. Barrie, "USS Gerald R. Ford: Inside the World's Most Advanced Aircraft Carrier," *FOX News*.

[16] A. Jenkins, "The Navy's New Aircraft Carrier, the USS Gerald Ford, Is the Most Advanced in the World," *Fortune*.

[17] P. Affairs, “Ready for the 21st Century,” *Navy.mil*.

[18] W. Weibull, “A Statistical Distribution Function of Wide Applicability,” *Journal of Applied Mechanics*, vol. 18, pp. 293–297, 1951.

[19] M. Xie and C. Lai, “Reliability Analysis Using an Additive Weibull Model with Bathtub-Shaped Failure Rate Function,” *Reliability Engineering and System Safety*, 1996.

[20] S. Usgaonkar and V. Mariappan, “Additive Weibull Model for Reliability Analysis,” *International Journal of Performability Engineering*, vol. 5, pp. 243–250, April 2017.

[21] C. Lai, M. Xie, and D. Murthy, “A Modified Weibull Distribution with Bathtub-Shaped Failure Distribution,” *IEEE Transactions on Reliability*, vol. 52, pp. 33–37, March 1996.

[22] G. Silva, E. Ortega, and G. Cordeiro, “A Beta Modified Weibull Distribution,” *Lifetime Data Analysis*, pp. 409–430, July 2010.

[23] S. Almalki and J. Yuan, “A New Modified Weibull Distribution,” *Reliability Engineering and System Safety*, vol. 111, pp. 164–170, 2013.

[24] A. Sarhan and J. Apaloo, “Exponentiated Modified Weibull Extension Distribution,” *Reliability Engineering and System Safety*, vol. 112, pp. 137–144, 2013.

[25] J. Berger and D. Sun, “Bayesian Analysis for the Poly-Weibull Distribution,” *Journal of the American Statistical Association*, vol. 88, pp. 1412–1418, 1993.

[26] M. Aarset, “How to Identify a Bathtub Hazard Rate,” *IEEE Transactions of Reliability*, vol. 36, pp. 106–108, 1987.

[27] J. Freels, “Modeling Reliability Growth in Accelerated Stress Testing,” 2013.

[28] E. Kreyszig, *Advanced Engineering Mathematics*. John Wiley and Sons, Inc., 2011.

Vita

Captain Daniel A. Timme graduated from Pearland High School in Pearland, TX. He began is collegiate career at San Jacinto Community College and then moving on to Univerisity of Houston where he earned a Bachelor of Science in Mathematics. He also attended University of Houston - Clear Lake where he simultaneously earned a Bachelor of Science in Business Management. Captain Timme earned his commission through Detachment 003 at University of Houston.

His initial training sent him to Fort Lee, VA where he earned a graduate certificate in Operations Research and Statistical Analysis - Military Applications Course (ORSA-MAC). His first assignment was to Barksdale AFB, LA working with Air Force Global Strike Command.He worked first as a Personnel and Systems Analyst with the AFGSC/A1 directorate and then moved on to become a Nuclear Systems Analyst with the AFGSC/A9 directorate. In August 2016, he was assigned to Wright-Patterson AFB, OH to attend Air Force Institute of Technology and pursue dual masters degrees in Systems Engineering with a focus in Reliability and Space Systems with focuses in Space Vehicle Design and Astrodynamics. Upon graduation, he will be assigned to 14 AF A5/8 /9 at Vandenberg AFB, CA.

REPORT DOCUMENTATION PAGE

Form Approved
OMB No. 0704–0188

The public reporting burden for this collection of information is estimated to average 1 hour per response, including the time for reviewing instructions, searching existing data sources, gathering and maintaining the data needed, and completing and reviewing the collection of information. Send comments regarding this burden estimate or any other aspect of this collection of information, including suggestions for reducing this burden to Department of Defense, Washington Headquarters Services, Directorate for Information Operations and Reports (0704–0188), 1215 Jefferson Davis Highway, Suite 1204, Arlington, VA 22202–4302. Respondents should be aware that notwithstanding any other provision of law, no person shall be subject to any penalty for failing to comply with a collection of information if it does not display a currently valid OMB control number. **PLEASE DO NOT RETURN YOUR FORM TO THE ABOVE ADDRESS.**

1. REPORT DATE *(DD–MM–YYYY)*	2. REPORT TYPE	3. DATES COVERED *(From — To)*
22–03–2018	Master's Thesis	Aug 2016 – Mar 2018

4. TITLE AND SUBTITLE

Modeling Multimodal Failure Effects of Complex Systems using polyWeibull Distribution

5a. CONTRACT NUMBER

5b. GRANT NUMBER

5c. PROGRAM ELEMENT NUMBER

6. AUTHOR(S)

Timme, Daniel A., Capt, USAF

5d. PROJECT NUMBER

5e. TASK NUMBER

5f. WORK UNIT NUMBER

7. PERFORMING ORGANIZATION NAME(S) AND ADDRESS(ES)

Air Force Institute of Technology
Graduate School of Engineering and Management (AFIT/EN)
2950 Hobson Way
WPAFB, OH 45433-7765

8. PERFORMING ORGANIZATION REPORT NUMBER

AFIT-ENV-MS-18-M-239

9. SPONSORING / MONITORING AGENCY NAME(S) AND ADDRESS(ES)

Office of the Secretary of Defense ATTN: Catherine Warner
1700 Defense Pentagon
Washington D.C., 20301
(703) 697-7247
Catherine.Warnerosd.mil

10. SPONSOR/MONITOR'S ACRONYM(S)

OSD DOT&E

11. SPONSOR/MONITOR'S REPORT NUMBER(S)

12. DISTRIBUTION / AVAILABILITY STATEMENT

Distribution Statement A. Approved For Public Release; Distribution Unlimited.

13. SUPPLEMENTARY NOTES

This work is declared a work of the U.S. Government and is not subject to copyright protection in the United States.

14. ABSTRACT

The DoD enlists multiple complex systems across each of their departments. Between the aging systems going through an overhaul and emerging new systems, quality assurance to complete the mission and secure the nation's objectives is an absolute necessity. The U.S. Air Force's increased interest in RPA and the Space Warfighting domain are current examples of complex systems that must maintain high reliability and sustainability in order to complete missions moving forward. DoD systems continue to grow in complexity with an increasing number of components and parts in more complex arrangements. Bathtub-shaped hazard functions arise from the existence of multiple competing failure modes which dominate at different periods in a systems lifecycle. The standard method for modeling the infant mortality, useful-life, and end-of-life wear-out failures depicted in a bathtub-curve is the Weibull distribution. However, this will only model one or the other, and not all three at once. The poly-Weibull distribution arises naturally in scenarios of competing risks as it describes the minimum of several independent random variables where each follows a distinct Weibull law. Little is currently known or has been developed for the poly-Weibull distribution. In this report, the poly-Weibull is compared against other goodness-of-fit models to model these completing multimodal failures. An equation to determine the moments for the poly-Weibull is derived leading to the development of properties such as the mean, variance, skewness, and kurtosis using MLE parameters obtained from a data set with known bathtub shaped hazard function.

15. SUBJECT TERMS

Reliability, Weibull, Test and Evaluation T&E, poly-Weibull, Statistics, Mathematics, Hazard Function, Bathtub Shape Hazard Function, Series, Parallel, System Reliability, Complex Systems, Derivation, Convergence, Density Function, Distribution Function, Maintainability, Survivability, Space Systems, Raw Moments, Mean, Standard Deviation, Variance, Skewness, Kurtosis, Expected Value

16. SECURITY CLASSIFICATION OF:			17. LIMITATION OF ABSTRACT	18. NUMBER OF PAGES	19a. NAME OF RESPONSIBLE PERSON
a. REPORT	b. ABSTRACT	c. THIS PAGE			Maj Jason K. Freels, PhD, AFIT/ENV
U	U	U	UU	109	19b. TELEPHONE NUMBER *(include area code)* (937) 255-3636 x4676 Jason.Freels@afit.edu

Standard Form 298 (Rev. 8–98)
Prescribed by ANSI Std. Z39.18